Marine and Petroleum Geology 75 (2016) 272–290

Contents lists available at ScienceDirect

Marine and Petroleum Geology

journal homepage: www.elsevier.com/locate/marpetgeo

Research paper

Late Cenozoic submarine slope failures in the southern North Sea – Evolution and controlling factors

Hauke Thöle [a, *], Gesa Kuhlmann [c], Rüdiger Lutz [b], Christoph Gaedicke [b]

[a] Institut für Geologie, Leibniz Universität Hannover, Callinstraße 30, D-30167 Hannover, Germany
[b] Federal Institute for Geosciences and Natural Resources, Stilleweg 2, D-30655 Hannover, Germany
[c] Federal Institute for Geosciences and Natural Resources, Wilhelmstraße 25-30, D-13593 Berlin, Germany

ARTICLE INFO

Article history:
Received 13 November 2014
Received in revised form
21 April 2016
Accepted 26 April 2016
Available online 28 April 2016

Keywords:
Mass transport deposits
Eridanos delta
Southern North Sea
Late Cenozoic

ABSTRACT

During the Late Miocene to early Pleistocene sedimentation in the southern North Sea Basin was dominated by a westward prograding depositional system. Progradation is evidenced by a series of large-scale, westward dipping clinoforms with amplitudes of up to 400 m. The clinoforms are related to a shelf-slope-basin physiography during deposition and their development and growth reflects the basinward migration of the Late Cenozoic shelf margin through time. Numerous submarine slope failures occurred on the shelf margin during this time, recognized as kilometer-scale mass-transport deposits (MTDs). Comparatively little is known about the earliest slope failures on this prograding shelf margin, yet their role is important in developing a coherent understanding of the origins of the instability of the margin as a whole. In this study we present detailed analyses of the first MTDs occurring on this Late Cenozoic shelf margin. Based on interpretation of 2D seismic reflection profiles, borehole data and integration of new chronostratigraphic datings the development and causes of slope instabilities are reconstructed. Three MTDs are distinguished within the German part of the southern North Sea, one (MTD1) that has been displaced in the Late Tortonian and two (MTD 2/3) in the Piacenzian. MTD 1 was triggered by salt-induced seismicity, as evident from salt-related faulting of the Late Cenozoic succession in its headwall domain. Pore pressure build up due to fluid migration from deeper levels in combination with loading imposed to the basin by the prograding shelf prism are the main factors controlling the initiation of MTDs 2 and 3.

Subsequent slope failures occurring during shelf progradation within the Dutch North Sea are much more frequent compared to the earliest slope failures. The development from a relatively stable shelf margin towards a margin affected by repeated slope failures coincides approximately with the intensification of Northern Hemisphere Glaciations during Pleistocene times. The development and deposition of the MTDs in the Dutch North Sea is clearly linked to climate-driven environmental changes, whereas prior to the Pleistocene failure mechanisms are preferably limited to those independent of glaciations and associated sea level changes and therefore fewer failures have occurred.

1. Introduction

Submarine slope failures are well known from areas dominated by high sediment supply (Hampton et al., 1996), such as along the fronts of rapidly prograding depositional systems ranging from deltas to continental margins. Failures of deltaic deposits have been largely documented both in modern and ancient examples, such as in the Mississippi delta (Prior and Coleman, 1978, 1982), in the Nidelva fjord delta (L'Heureux et al., 2009), in the Eocene Sobrabre delta complex (Callot et al., 2009), in the Gulf of Mexico (Perov and Bhattacharya, 2011) and in a Middle Miocene delta within the Roer Valley Graben (Deckers, 2015). Sediment instabilities are also an intrinsic facet of numerous larger-scale progradational systems, including the Lower Cretaceous Torok Formation on the North Slope of Alaska (Kerr, 1985; Homza, 2004), the Cenozoic clinoforms offshore New Jersey (McHugh et al., 1996, 2002), the post-Messinian succession of the Israeli continental margin (Frey-Martinez et al., 2005) and the Pleistocene slope succession of the Pescara Basin (Dalla Valle et al., 2013).

Within the southern North Sea Basin several slope failures have

* Corresponding author.
E-mail address: thoele@geowi.uni-hannover.de (H. Thöle).

http://dx.doi.org/10.1016/j.marpetgeo.2016.04.028

been recognized within the Late Cenozoic sedimentary succession (Cameron et al., 1993; Sørensen et al., 1997; Overeem et al., 2001; Benvenuti et al., 2012). At this time, the sedimentation was dominated by a westward prograding depositional system, often referred to as the 'Eridanos delta' (Overeem et al., 2001). Progradation is evidenced by a series of large-scale, westward dipping clinoforms with amplitudes of up to 400 m. In spite of its common denomination as 'delta', the heights of these clinoforms, however, indicate that these landforms actually represent a prograding shelf margin. Clinoforms created by deltas are typically only 10 s of meters high (e.g. Johannessen and Steel, 2005; Helland-Hansen and Hampson, 2009) and should not be confused with the clinoforms described in this study, which are 100 s of meters observed on 2D seismic data. The scale of the seismic clinoforms is referred to as shelf-margin clinoforms by many workers (Steel and Olsen, 2002; Bullimore et al., 2005; Johannessen and Steel, 2005; Helland-Hansen and Hampson, 2009). Prograding systems of similar size (thickness of clinoforms, ~200–500 m) are described e.g. in the Central Tertiary Basin of Spitsbergen (Johannessen and Steel, 2005), Porcupine Basin of offshore Ireland (Johannessen and Steel, 2005; Ryan et al., 2009), West Siberian Basin of Russia (Pinous et al., 2001), western Barents Sea (Glørstad-Clark et al., 2010, 2011) and Dacian Basin of Romania (Fongngern et al., 2015).

Progradation of the 'Eridanos delta' developed mainly from the Northeast and East and subsequently from the Southeast leading to deposition of the oldest sequences in the eastern most part of the Danish and German North Sea sector and increasingly younger sequences towards the west (Michelsen et al., 1998; Thöle et al., 2014). Most of the slope failures are found within the youngest portion of the prograding shelf prism within the Dutch part of the southern North Sea (Fig. 1) and are dated to, or presumed to be of Late Pliocene to Pleistocene age (Benvenuti et al., 2012). They have been described in detail by Benvenuti et al. (2012), who suggested that the main precondition for these instabilities is related to the interplay between high sediment supply and constant or even decreasing accommodation space caused by glacioeustatic sea level fall. In places where salt domes are found, Benvenuti et al. (2012) considered salt-induced seismicity and upward fluid escape as important triggers for slope failure.

However, no details have been reported yet about the earliest slope failures that occurred when the main depocentre of the prograding system was located more to the east, i.e. in the German North Sea sector (Thöle et al., 2014). Instabilities are less frequent and extensive compared to the Dutch North Sea sector, yet their role is important in developing a coherent understanding of the origins of the instabilities of the prograding shelf margin as a whole.

The aim of this paper is to present a detailed description of the earliest slope failures that occurred on the shelf margin and to reconstruct the history of slope instability in the area of the southern North Sea during Late Cenozoic times. 2D seismic reflection profiles have been interpreted together with new chronostratigraphic datings to discuss the timing of the submarine slope seen in the German North Sea sector with respect to the development of the prograding system, as well as their relation to the slope failures found in the Dutch sector of the southern North Sea. The role of different geological processes contributing to slope failure, such as fluid migration, salt movements and sedimentation history, will be discussed.

2. Geological setting

The study area is situated in the southern part of the present day North Sea and comprises the western part of the German offshore territory (Fig. 1). The North Sea has had a long and complex geological history and its present-day structural configuration is largely the result of Late Jurassic to Early Cretaceous rifting, followed by a phase of post-rift thermal subsidence during later Cretaceous and Cenozoic (Ziegler, 1992; Glennie and Underhill, 2009). During most of the post-rift phase the basin thermally subsided and was filled with sediments sourced from the surrounding landmasses, interrupted periodically by basin inversion (e.g. Vejbaek and Andersen, 1987; Ziegler, 1990; de Lugt et al., 2003; Rasmussen, 2009).

During Cenozoic times more than 3 km of siliciclastic sediments accumulated in the North Sea area with the main depocentre above the Central Graben (Ziegler, 1990). Half of these sediments were deposited during post-Mid Miocene time. During this interval, the southern part of the North Sea became the depocentre of a large westward prograding depositional system – often referred to as the Eridanos delta (sensu Overeem et al., 2001). Progradation is evidenced by a series of large-scale, westward dipping clinoforms with amplitudes of up to 400 m. The clinoforms are related to a shelf-slope-basin physiography during deposition and their development and growth reflects the basinward migration of the Late Cenozoic shelf margin through time. The evolution of the entire sedimentary system and several parts of it has been the subject of numerous publications (e.g. Cameron et al., 1993; Sørensen et al., 1997; Overeem et al., 2001; Kuhlmann, 2004; Rasmussen et al., 2005; Møller et al., 2009; Knutz, 2010; Benvenuti et al., 2012; Stuart and Huuse, 2012; Thöle et al., 2014).

The shelf margin system built out from the eastern seaboard into the North Sea and progressively prograded towards the west. The sediments were mainly delivered into the basin by the Baltic River System, a former fluvial system that drained most of the Fennoscandian and Baltic Shield between Late Oligocene and Early Pleistocene times (Bijlsma, 1981). The deposition of the 'Eridanos delta' started in the Late Miocene, and it is separated from the upper Palaeocene to middle Miocene succession by a major unconformity, called the Mid-Miocene Unconformity (MMU, Michelsen et al., 1998). On seismic profiles the unconformity appears as a prominent downlap surface within the southern North Sea region, separating largely concordant sedimentary sequences underneath, from sediments shed into the basin by the prograding system (Köthe, 2007). The interval below the MMU consists mainly of deep-marine, relatively fine-grained siliciclastic sediments (predominately clays) of upper Palaeocene to lower Middle Miocene age (Köthe, 2011), which are deformed basin-wide by polygonal faulting caused by volumetric contraction of the muddy, smectite-rich sediments during early burial (Cartwright, 1994; Cartwright and Lonergan, 1996). Above the MMU smectite amounts decrease (Dewhurst et al., 1999) and the package consists of mainly clay and silt, locally intercalated with sand-rich layers deposited as well-developed clinoforms.

A large number of salt structures (pillows, walls and diapirs), belonging mainly to the Zechstein Group, are present in the southern North Sea Basin (e.g. Reinhold et al., 2008). These structures locally influenced the Cenozoic sedimentary succession (e.g. Korstgård et al., 1993; Remmelts, 1996: Brückner-Röhling et al., 2005), as seen among others from a relatively irregular topography of the Mid-Miocene Unconformity (MMU; Fig. 1).

Increased clastic influx and related westward progradation of the shelf margin is commonly explained as result of accelerated uplift of the Fennoscandian shield, coupled with a marked deterioration in climate that began in the middle Eocene, reflecting progressive expansion of the Antarctic ice shield (Knox et al., 2010; Eidvin et al., 2014). The sedimentation pattern established since the Late Miocene – with the dominant sediment supply from the Baltic river system – persisted until the Mid-Pleistocene (Overeem et al., 2001; Westerhoff, 2009). Then the onset of repeated glaciations at

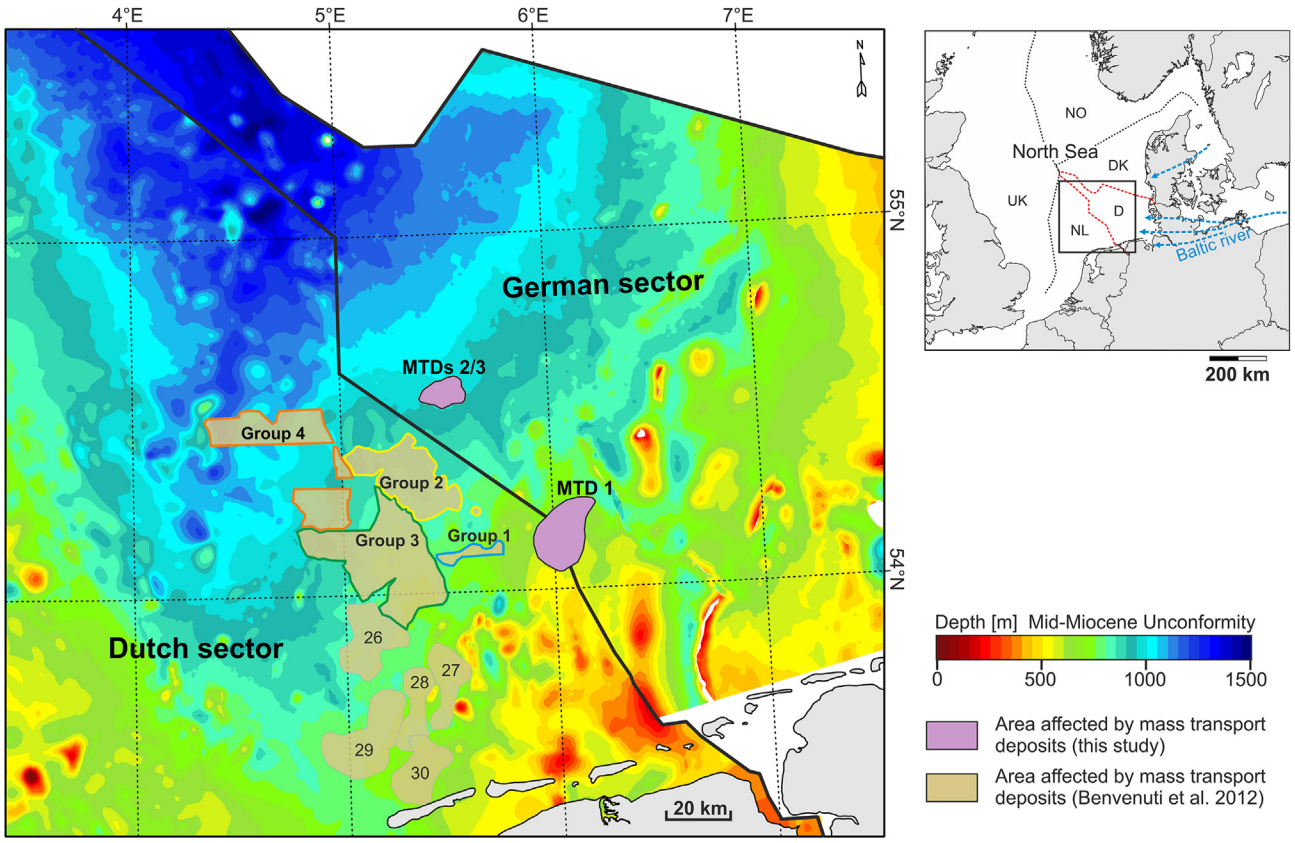

Fig. 1. Map of the study area in the southern North Sea showing the distribution of Late Cenozoic MTDs identified in this study and by Benvenuti et al. (2012) with superimposed time-structure map of the Mid-Miocene Unconformity (MMU). For the Dutch offshore sector, the MMU is derived from the TNO database of the deep subsurface (www.nlog.nl) and for the German offshore sector from Thöle et al. (2014). Particular in the southern and southeastern part of the Dutch and German North Sea sectors, the MMU is pierced and uplifted by various salt diapirs and fault systems, showing post Mid-Miocene salt movements.

the headlands of the Baltic river system finally destroyed the river system and the easterly-sourced progradation ended.

3. Database and methodology

3.1. Definition of mass transport deposits

Many different classification schemes exist for submarine slope failures, and specific nomenclature often differs between studies (Richardson et al., 2011, and references therein). In this paper we use the generic term “mass transport deposits” (MTDs) to describe sediments affected by submarine slope failures (e.g. Posamentier and Martinsen, 2011; Richardson et al., 2011). MTDs encompass a wide spectrum of gravity-induced deposits. They include movement and emplacement by brittle deformation (slides), plastic deformation (slumps), and plastic or laminar flow (debris flows), but generally exclude turbidities (Nelson et al., 2011). Depending on the kind of mass movements they can be associated with various geometries and seismic facies (Bull et al., 2009). The different seismic expressions of MTDs are well documented by numerous studies, e.g. Frey-Martinez et al. (2005, Frey-Martínez et al., 2006; 2011), Moscardelli et al. (2006), Bull et al. (2009), and Posamentier and Martinsen (2011). According to these studies, MTDs are generally recognized on seismic data as discrete bodies which exhibit a highly disrupted to chaotic internal structure representing the failed mass. Extensional structures (e.g. normal and listric faults) generally dominate the upslope parts of an MTD, while compressional features (e.g. folds and thrusts) usually dominate the downslope areas (e.g. Bull et al., 2009; Frey-Martínez, 2010). The lower boundary of a MTD is defined by a basal shear surface. This surface separates the failed and translated mass from the underlying, undeformed strata, and corresponds to a stratigraphic layer where the downslope-oriented shear stress exceeds the shear strength of the sediment (Frey-Martínez, 2010). The basal shear surface often forms a continuous plane that dips parallel to the underlying strata. However, as shown in Frey-Martinez et al. (2005), it may locally ramp up and down to form a step-like geometry. The upper surface of a MTD is usually irregular, indicating the bathymetry after the time of erosion. Undeformed sediments above the MTDs are indicative for the timing of MTD formation.

3.2. Database

The MTDs described in this study are mapped and analyzed on the basis of four commercially acquired 2D seismic reflection surveys (AR-EHJK-91, G2002, G85 and GR86). The dominant frequency of the seismic datasets varies between 35 and 45 Hz within the interval of interest, providing a theoretical vertical resolution (defined as a quarter of the dominant wavelength, $\lambda/4$) of c. 11–14 m, based on an average sediment velocity equal to 2 km/s. In addition, further regional seismic surveys covering the German and the Dutch North Sea sector have been used for this study (Fig. 2). These datasets provided a broader perspective of the study area and a context for the detail study of the MTDs. The seismic dataset has been further complemented with gamma-ray and sonic logs of nearby exploration boreholes (Fig. 2), whereby no well directly intersects one of the studied MTDs.

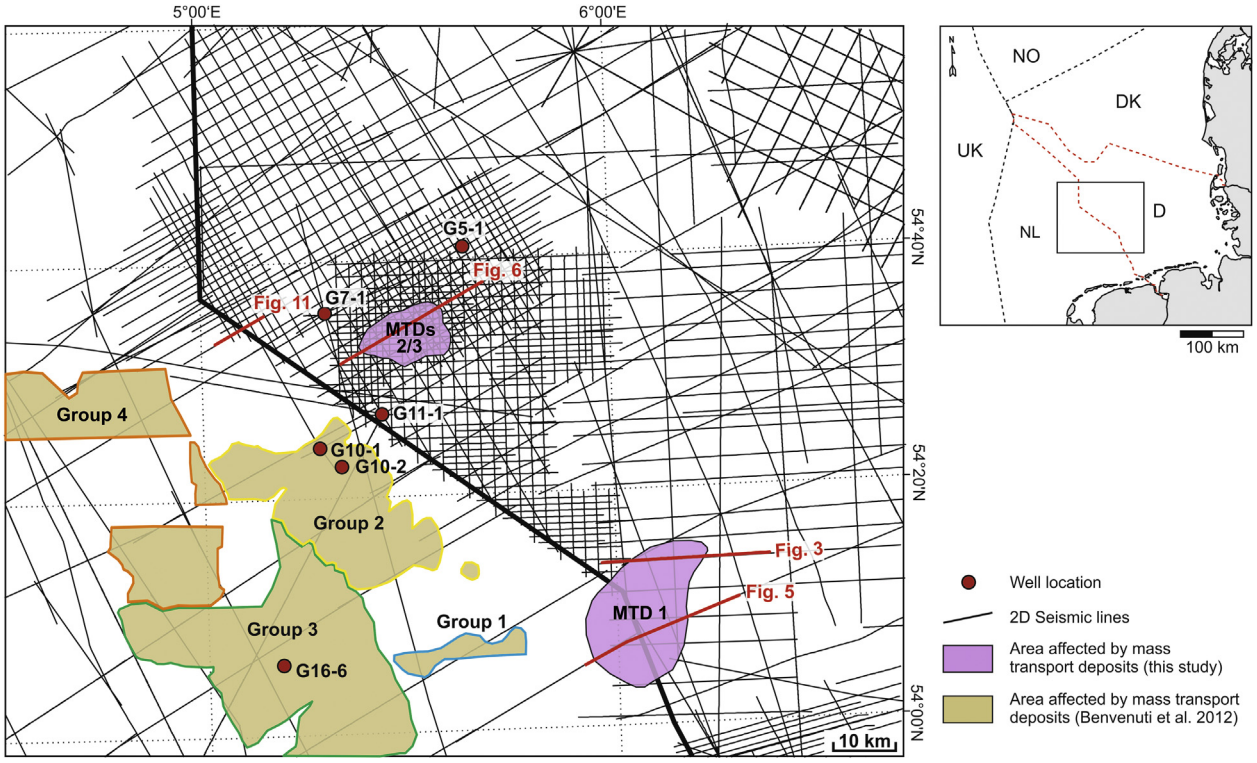

Fig. 2. Detail map of seismic lines used in the study as well as locations of explorations wells referred to in text. Also marked are Late Cenozoic MTDs recognized in this study and by Benvenuti et al. (2012). Red solid lines indicate the location of seismic profiles shown as figures. Line spacing in the area of MTDs 2 and 3 is between 200 m and 1000 m. In the area of MTD 1 the line spacing is approx. between 2000 m and 4000 m. (For interpretation of the references to color in this figure legend, the reader is referred to the web version of this article.)

3.3. Methodology

All seismic interpretations, as well as subsequent well-log analyses, were carried out on a UNIX seismic workstation using the GeoFrame® software package of Schlumberger. Seismic profiles were used to map the extent of the MTDs, to analyze their architecture and relationships with underlying and peripheral sedimentary units, as well as the nature of their basal contact. Interpretation of failure and transport processes is based on morphological characteristics and lateral and vertical changes in seismic facies.

In order to place the mass failures into the geological context, the seismic-stratigraphic framework established by Thöle et al. (2014) has been used. This framework subdivides the post-Mid Miocene succession of the German part of the southern North Sea Basin into seven seismic units (SU1-SU7), which are separated by distinct seismic surfaces (MMU, H1-H7) that represent major depositional or erosional boundaries (Table 1). The age of the seismic units were constrained by biostratigraphic studies on dinocyst assemblages from four wells (B-15-3, G-5-1, G-11-1, J-5-1) in the German North Sea sector (Köthe, 2011) and by the Tove-1 well in the Danish North Sea (Dybkjær and Piasecki, 2010).

4. Results

Three MTDs are recognized within the Late Cenozoic sedimentary succession of the German North Sea sector based on 2D seismic data. The individual MTDs, numbered progressively from the oldest (MTD 1) to the youngest (MTD 3), are imaged on seismic profiles as km-scale sedimentary bodies, characterized by seismic facies made up of highly discontinuous to chaotic reflectors. In the following we describe the general stratigraphic context of the MTDs together with the overall internal and external characteristics of the MTDs, with their vertical and lateral structural changes, and relationships with the host sedimentary succession. Furthermore, seismic indications for shallow gas and fluid flow observed within MTDs 2 and 3 and in their vicinity have been described.

4.1. Mass transport deposit 1 (Late Tortonian)

4.1.1. General characteristics and seismic stratigraphic position

One slope failure has been identified within the upper part of seismic unit SU3 (Fig. 3). Sediments within this unit have been dated approximately from their palynology as Late Tortonian (Thöle et al., 2014, Table 1) and exhibit a strong progradational character with steeply dipping clinoforms. The top of unit SU3 is formed by horizon H3 and is unaffected by the slope failure. This horizon is of late Tortonian to early Messinian age and MTD1 is thus not younger than early Messinian. Intact clinoforms next to the mass transport deposit are characterized by complex sigmoidal-oblique to oblique tangential foreset geometries with no or poorly developed topsets, as indicated in Fig. 4. Towards the North, away from the MTD the inclination of the clinoforms decreases, forming longer and more gently dipping sigmoidal foresets.

The deposit of the slope failure (MTD 1) extends from the southwestern part of the German offshore block H into the Dutch North Sea sector (Fig. 4). It has a maximum length of approximately 25 km and its width is progressively increasing from 4 km in the Northeast to more than 15 km in the Southwest, covering an area of approximately 280 km^2. The average thickness is 150 ms (TWT), with a maximum depth to detachment of 200 ms (TWT).

Table 1
Stratigraphic position of the mass transport deposits group 1 to 4 and MTDs 26 to 30 as documented by Benvenuti et al. (2012) in relation to the MTD 1 and MTDs 2/3 described in this study.

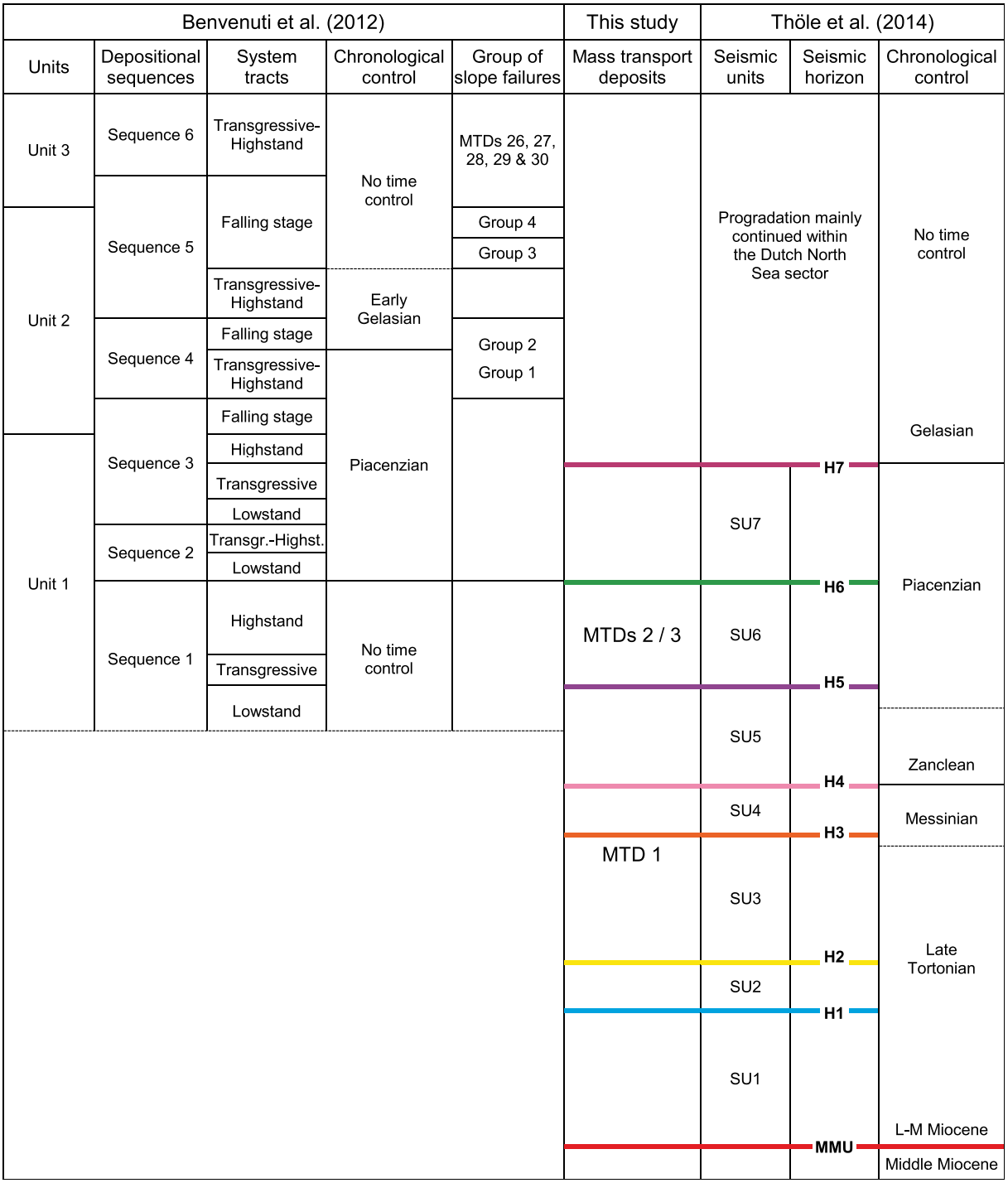

4.1.2. Basal shear surface

The base of MTD 1 is imaged as a planar to highly irregular surface and runs along multiple reflections, which are located at different stratigraphic levels. Over large areas of the MTD, the basal shear surface is located within the underlying Paleogene sediments slightly below the MMU and forms a corrugated irregular surface that maintains roughly parallel to the underlying strata (Fig. 5). This configuration changes in the westerly, proximal part of the MTD, where the basal shear surface cuts up section and often corresponds to the base of a clinoform (Figs. 3 and 5).

4.1.3. Internal geometry and shape

Internally, MTD 1 exhibits a complex geometry dominated by folding and intense faulting (Fig. 5), whereby individual blocks of the MTD have retained a high degree of internal coherency. Down with the length of the MTD a distinctive longitudinal

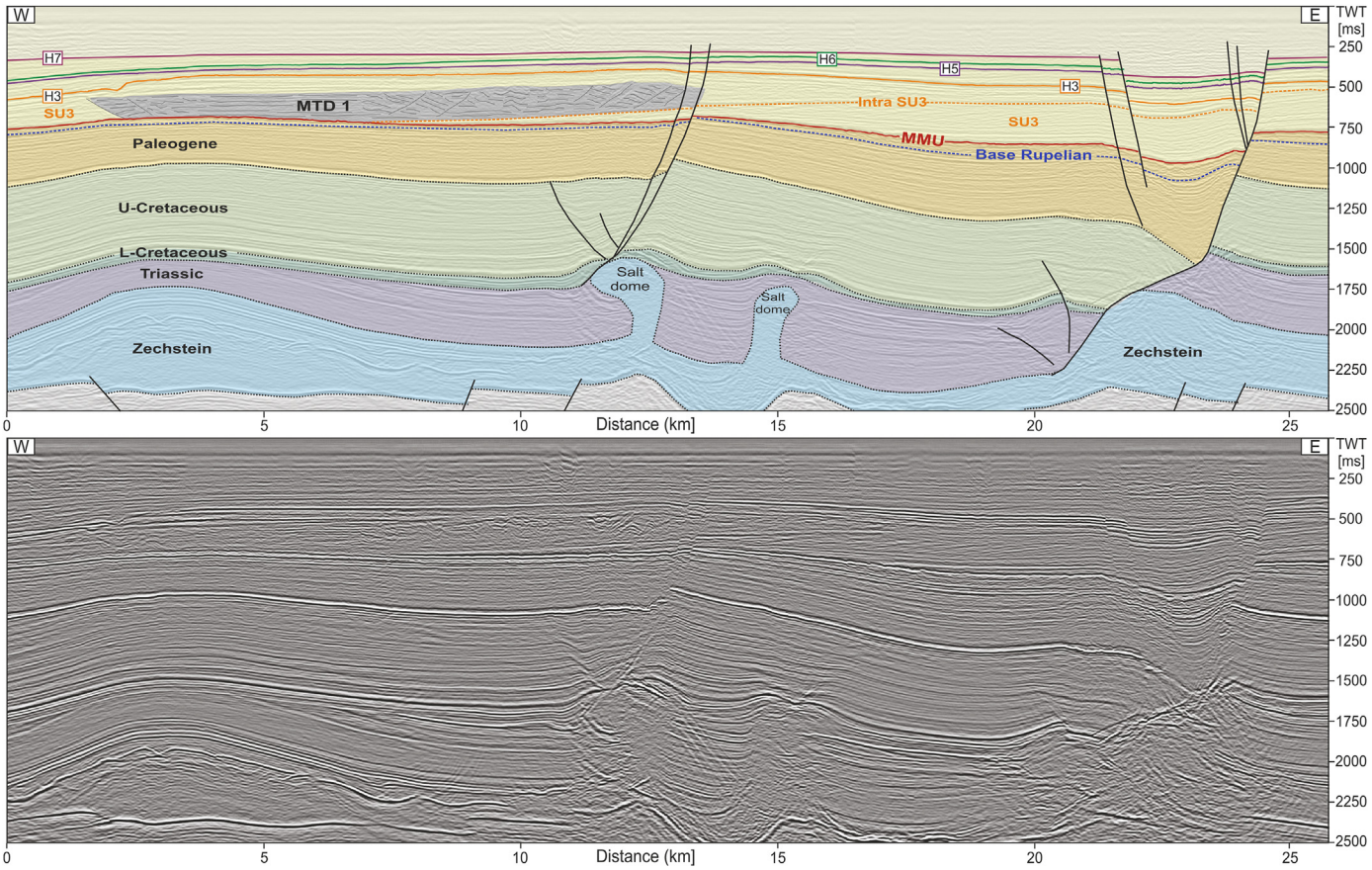

Fig. 3. Interpreted (upper panel) and uninterpreted (lower panel) 2D seismic reflection profile, oriented southwest-northeast, showing the general stratigraphic position of MTD 1 in the Late Cenozoic sedimentary succession and its relationship to deeper structures. Note the presence of salt-related faults affecting the headwall domain of MTD 1 as well as adjacent sediments. Location of seismic profile is given in Fig. 2.

transformation in the structural style can be observed. The eastern most, proximal part of the MTD is dominated by normal faults, followed by a segment that shows no clear dominance of either extensional or compressional deformation. The internal structure of this segment, covering the central part of the MTD, is mainly characterized by folding and sets of conjugate faults that are contractional as well as extensional in origin. Extensional faulting manifested as both horst-and-graben structures and tilted blocks as well as reverse faults associated with folds and pop-up structures can be observed along the entire length in this part of MTD 1 (Fig. 5), whereby with increasing distance downslope reverse faults become prevalent. Near the frontal parts of the toe region, MTD 1 runs onto a local slope and shows a prevalence of thrust-related deformation (Fig. 5). It is inferred that the thrusts faults, visible as steeply dipping parallel reflections on seismic sections, were formed due to the topographic feature, which may acted as barrier to the NE-SW flowing mass.

4.2. Mass transport deposits 2 and 3 (Piacenzian)

4.2.1. General characteristics and seismic stratigraphic position

Two MTDs of apparently slightly differing age have been identified within the German offshore Block G8 (Fig. 6). These MTDs (named MTD 2 and 3) exhibit a number common characteristic and will be described together. They are located both within seismic unit SU6, which has been dated approximately from its palynology as Piacenzian (Thöle et al., 2014, Table 1). Numerous internal discontinuities of variable lateral extent have been observed within this unit. Few of them can be mapped regionally allowing a further subdivision of seismic unit SU6 into at least 3 subunits (SU6.1-SU6.3; Fig. 6). Intact clinoforms next to the MTDs are characterized by complex sigmoidal-oblique to oblique tangential foreset geometries with no or poorly developed topsets (Fig. 7).

The older of the two MTDs (MTD 2), located within subunit SU6.2, has a maximum width of 8 km and is a least 9 km long, affecting an area of approximately 75 km^2. The average thickness is 350 ms (TWT), with a maximum depth to detachment of 480 ms (TWT). The deposit of the younger slope failure (MTD 3) is located within subunit SU6.3 and covers an area of approximately 35 km (mean length 6 km, mean width 6 km). Its average thickness is ca. 400 ms (TWT), increasing to a maximum of ca. 530 ms (TWT) in its upper part.

4.2.2. Basal shear surface

MTDs 2 and 3 share the same basal shear surface, a key observation in terms of slope failure processes that is discussed in more detail later. In contrast to MTD 1 where predominately post-Mid Miocene sediments were affected by the slope failure (Figs. 3 and 5), the detachment surface at the base of MTDs 2 and 3 is located at a deeper stratigraphic level within the underlying Paleogene succession (Fig. 6). The relatively fine-grained sediments of the Paleogene are deformed basin-wide due to polygonal faulting (Cartwright, 1994; Cartwright and Lonergan, 1996), whereby the intensity of faulting varies with depth (Fig. 8). Over large areas of the MTDs, the basal shear surface corresponds to a distinct and continuous horizon. This horizon approximately coincides with the base of the Rupelian from its palynology (Köthe, 2007, 2011) and separates intervals of varying polygonal-faulting. The seismic

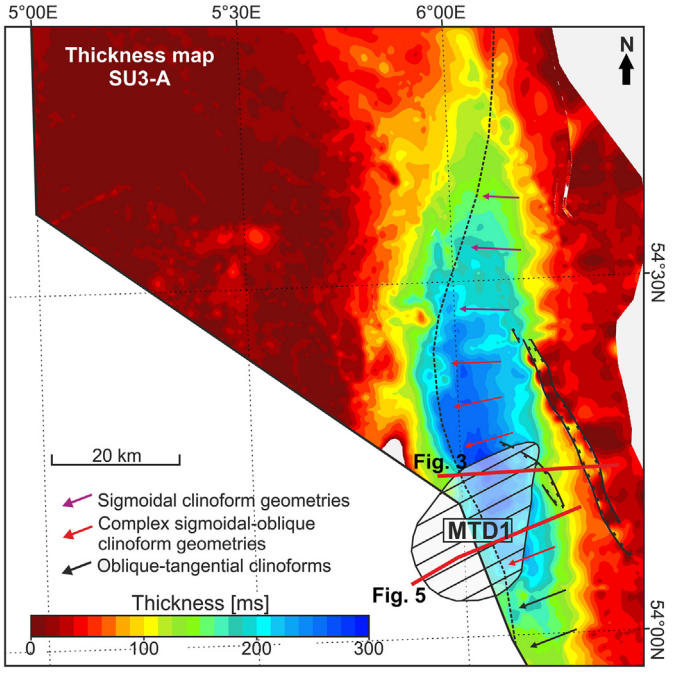

Fig. 4. Thickness map of the uppermost part of seismic unit SU3, showing the position of the main depocentre during the earliest slope failure (MTD 1). The displayed thickness corresponds to the interval between intra SU3 and horizon H3, indicated in Fig. 3. The areal extent and spatial distribution of different clinoform geometries are marked by the arrows. Stippled line indicates the final position of the clinoform breakpoint within unit SU3.

section shown in Fig. 8 illustrates the stratigraphy and structure of the fault system in the vicinity of well G-11-1 which is located close to MTDs 2 and 3. The interval between MMU and base Rupelian is recognized as a generally high-amplitude interval that is subject to intense polygonal faulting, whereas below the base Rupelian within the Eocene succession less intense faulting and typically lower amplitude reflections can be observed (Fig. 8). The significant change between the two intervals may be caused by lithological differences. This interpretation is supported by observations from well logs from nearby wells (G-5-1, G-7-1 and G-11-1), which show a conspicuous log break on the gamma-ray logs. The boundary between the intervals is recognized on the gamma-ray logs by a change from generally decreasing gamma-ray values towards an upward increasing log response (Fig. 8).

The base Rupelian acting as the main basal shear surface has been mapped within the vicinity of the MTDs. The corresponding time-structure map (Fig. 8) shows that the detachment surface at the base of MTDs 2 and 3 is centered above the crests of positive topographic features. These topographic highs are primarily controlled by the presence of underlying salt structures. As illustrated by Fig. 6, the investigated MTDs are located above two salt domes (Gracia in the west and Gloria in the east), which bent upwards the overlying sediments forming a positive structural relief associated with domal/anticlinal structures.

4.2.3. Internal geometry and shape

MTDs 2 and 3 show many of the same characteristic features but also some differences in their seismic appearance (Fig. 9). Throughout the upslope region of the MTDs, extensional structures are prevalent. Deformation is here mainly dominated by listric faults forming a series of rotational blocks that are tilted updip. Most of the associated listric faults sole out at the basal shear surface of the MTDs. The rotated blocks have largely maintained their original internal stratification, pointing to a low degree of disintegration and of a relatively modest downslope transfer of sediment. Both MTDs are only slightly depressed with respect to the undeformed region of the slope, suggesting a very limited depletion of sediments (Fig. 9).

With increasing distance downslope from the headwall scarps, structures become more subdued, showing a complex internal geometry with no clear dominance of either extensional or compressional deformation. Folds and thrust structures as well as rotated and/or deformed blocks of coherent strata seem to be present (Fig. 9). Pop-up like structures can be recognized over the entire MTD's length. In parts, the MTDs are dominated by low coherence seismic facies coinciding with intensively deformed sediments that have little to no original stratification preserved in the seismic character.

An additional and important observation regarding the internal seismic architecture of the MTDs is that both have developed a frontal ramp where the basal shear surface climbs up sections. MTD 2 is characterized by a frontal ramp along which the displaced mass is translated above the paleo-seafloor (Fig. 9) and is thus an example of a frontally emergent landslide as classified by Frey-Martínez et al. (2006). While MTD 3 can be classified as a frontally confined landslide (sensu Frey-Martínez et al., 2006) as it has a relatively steep frontal ramp along which the displaced mass is buttressed against the undeformed stratigraphic section (Fig. 9).

4.3. Seismic indications for shallow gas and fluid flow

Seismic indications for shallow gas and fluid migration have been observed within MTDs 2 and 3 and in their vicinity. As seen in Fig. 10, significantly increased seismic amplitudes compared to adjacent horizons have been recognized at the top of these MTDs and also in part below their depositional area. These high amplitude anomalies characterized by distinct local brightening of the sedimentary reflections may indicate a significant change in acoustic impedance. Since the early 1970s amplitude anomalies have been assisted as direct hydrocarbon indicators in the oil and gas exploration (Sheriff and Geldart, 1995). The presence of gas within sediments has a strong decreasing effect on the acoustic impedance (e.g. Domenico, 1976). This will generally lead to negative amplitude anomalies at the top of the gas. However, our seismic data do not allow to determine the polarity of these seismic events, as the high amplitudes are not restricted to a single reflector. Nevertheless, the observed high amplitude anomalies with their local extent strongly suggest that these anomalies are caused by gas in the sediments and in the following we refer to these reflections as gas-related amplitude anomalies. This is supported by the fact that shallow gas is encountered widely in the southern North Sea, and occurs even in commercial quantities in the northern part of the Dutch offshore sector (Pletsch et al., 2010).

Seismic indications for fluid migration are provided by numerous mounded structures that have been observed in the vicinity of MTDs 2 and 3. The mounds occur in seismic unit SU6 and are developed on top of the MMU (Fig. 11). In size, they are up to 100 ms (TWT) high and have an internal reflection pattern of convex-upward reflections that downlap and terminate onto the MMU. In some cases the stratal reflections immediately underneath these features are downthrown, resulting in the development of a sag-like structure underlying the main part of the mounded structures, while overlying strata displays onlap onto the mounds (Fig. 11). The mounded structures appear to be preferentially developed above underlying salt structures and seem partly to be connected via faults to them. The relation between mounds and salt domes is illustrated on several seismic sections (Fig. 11).

A variety of geological processes may result in mound shaped

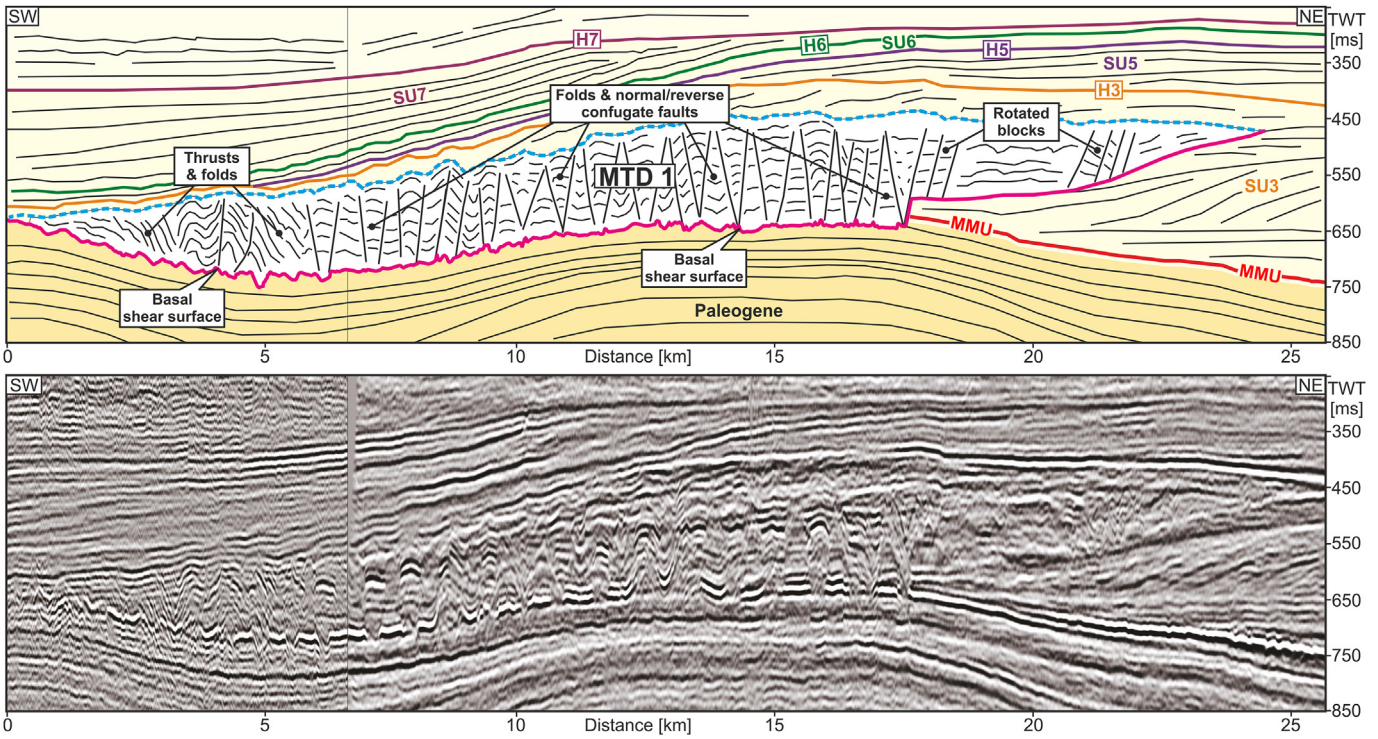

Fig. 5. Interpreted (upper panel) and uninterpreted (lower panel) 2D seismic reflection profile, oriented southwest-northeast, showing the internal architecture of MTD 1 which is characterized by intense faulting and folding. The base of MTD 1 is mainly located slightly below the MMU within the underlying Paleogene sediments, where it forms a corrugated irregular surface. Towards the Northeast, the basal shear surface cuts up section and coincide with the base of a clinoform. Location of seismic profile is given in Fig. 2. Seismic data provided by TGS-NOPEC.

morphological features on the seafloor (Andresen et al., 2009, and references therein). Benvenuti et al. (2012) recognized similar features in the Dutch North Sea sector and suggested that sediment-laden fluids ejected by salt domes created those mounds. Several examples of sand extrusions, referred to as extrudites, have been described for the Cenozoic North Sea Basin (Andresen et al., 2009; Løseth et al., 2012). These studies illustrate that sand extrusion may produce mounded structures of similar scale and with similar reflection configuration (basal downlap, external onlap), as the ones observed here on top of the MMU. Given the available information a likely interpretation of the mounds as sand/mud extrusions can be made, but other origins such as contourites cannot be ruled out.

5. Discussion

5.1. Timing of Late Cenozoic MTDs in the southern North Sea

The MTDs described in this paper are part of a series of slope instabilities affecting the front of the rapidly prograding Late Cenozoic shelf margin in the southern North Sea (Sørensen et al., 1997; Overeem et al., 2001; Benvenuti et al., 2012). As illustrated by the clinoform breakpoint migration map (Fig. 12), shelf margin progradation developed mainly from the Northeast and East leading to deposition of the oldest sequences in the easternmost part of the Danish and German North Sea sector and increasingly younger sequences towards the west. Most of the slope failures are found within the youngest portion of the prograding system within the Dutch part of the southern North Sea and have been described in detail by Benvenuti et al. (2012). They mapped and analyzed 30 MTDs and divided them into four groups from younger to older (Group 1 to 4), whereby the youngest MTDs 26 to 30 are not part of group, since they are more randomly distributed (Fig. 1).

Table 1 shows the stratigraphic position of the mass transport deposits documented by Benvenuti et al. (2012) in relation to the MTDs described in this study. Benvenuti et al. (2012) dated the deposits and associated MTDs in the Dutch North Sea based on biostratigraphic analysis from four wells (G10-1, G10-2, G16-6 and MO7-1; Fig. 2), whereby no exact time control exists for their younger MTDs from group 3 and above (Table 1). For the MTDs of their group 1 and 2 Benvenuti et al. (2012) proposed a Piacenzian to early Gelasian age. Our chronology, which is based on the seismo-stratigraphic framework of Thöle et al. (2014), reveal younger ages for the MTDs of group 1 and 2 than the one Benvenuti et al. (2012) suggested (Table 1).

Thöle et al. (2014) proposed a Piacenzian age for their seismic unit SU7, whereby the upper boundary (horizon H7) corresponds to the Pleistocene/Pliocene boundary defined at 2.59 Ma, equivalent to Top Piacenzian, following the Geological Time Scale 2012 (GTS2012; Gradstein et al., 2012). This age is in agreement with the chronostratigraphic framework established by Kuhlmann et al. (2006) for the Late Cenozoic sedimentary succession in the northern Dutch offshore sector. The boundary of their seismic units S4 and S5 (equivalent to our top SU7; Thöle et al., 2014) coincides with the paleomagnetic Gauss-Matuyama boundary at around 2.6 Ma (Kuhlmann and Wong, 2008), which roughly corresponds to the Pleistocene/Pliocene boundary. Compared to the study of Benvenuti et al. (2012), the upper boundary of SU7 correlates in seismic profiles with the transgressive/highstand system tract boundary of their sequence 3 (Table 1). According to Benvenuti et al. (2012) this sequence as well as parts of their sequence 4 has been dated as Piacenzian, whereas our chronology suggests slightly younger ages. Since our age for the upper boundary of SU7 match very well with the results obtained by Kuhlmann and Wong (2008),

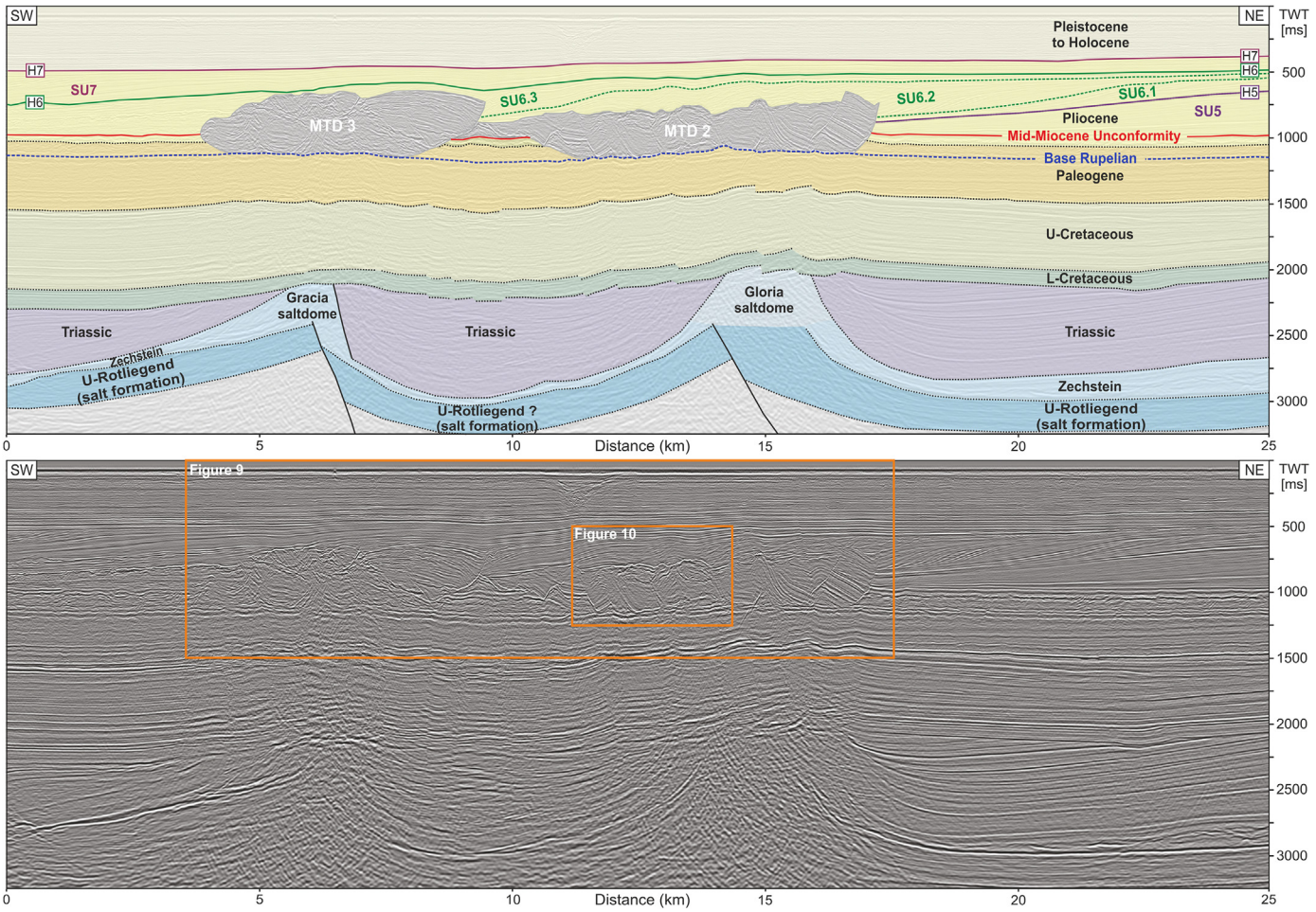

Fig. 6. Interpreted (upper panel) and uninterpreted (lower panel) 2D seismic reflection profile, oriented southwest-northeast, showing the general stratigraphic position of MTDs 2 and 3 in the Late Cenozoic sedimentary succession and its relationship to deeper structures. The two MTDs of apparently slightly differing age share the same basal shear surface, which approximately coincides with the base of the Rupelian. Seismic interpretation beneath the MTDs is challenging because they dramatically affect the seismic signal. Faults probably related to salt structures are difficult to distinguish from seismic artefacts. Location of seismic profile is given in Fig. 2. Seismic data provided by TGS-NOPEC.

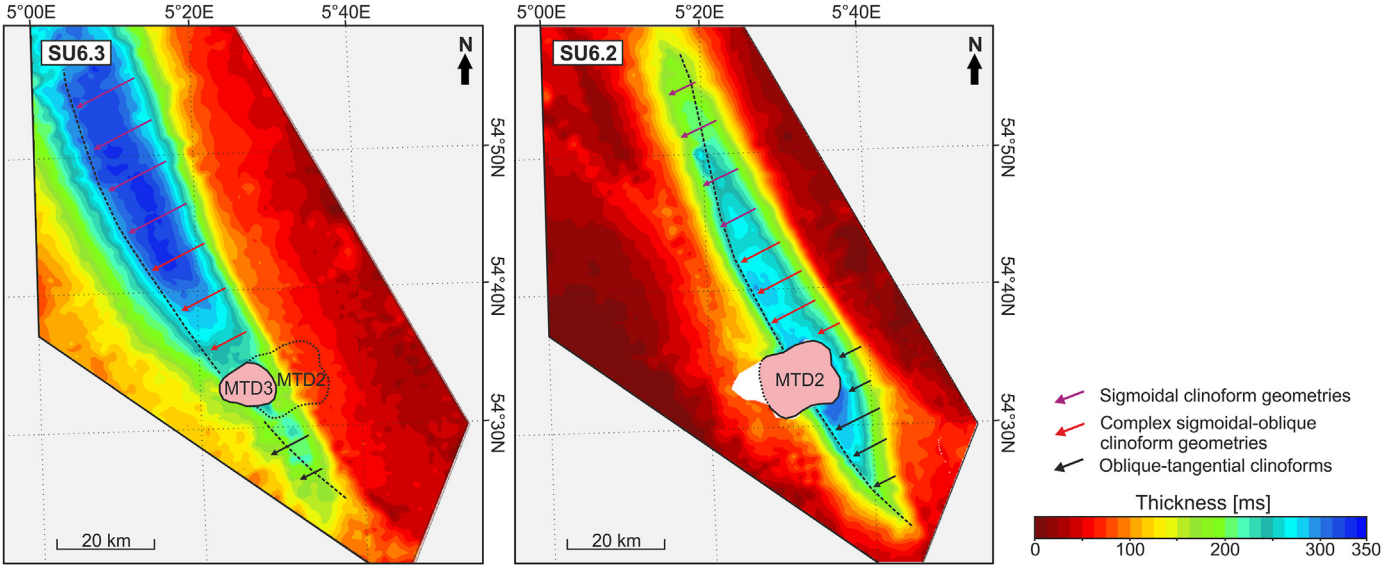

Fig. 7. Thickness maps of seismic subunits SU6.2 and SU6.3, showing the position of the depocentre during formation of MTDs 2 and 3. The corresponding subunits are marked in Fig. 6. The areal extent and spatial distribution of different clinoform geometries are marked by the arrows. Stippled line indicates the final position of the clinoform breakpoint within unit SU3.

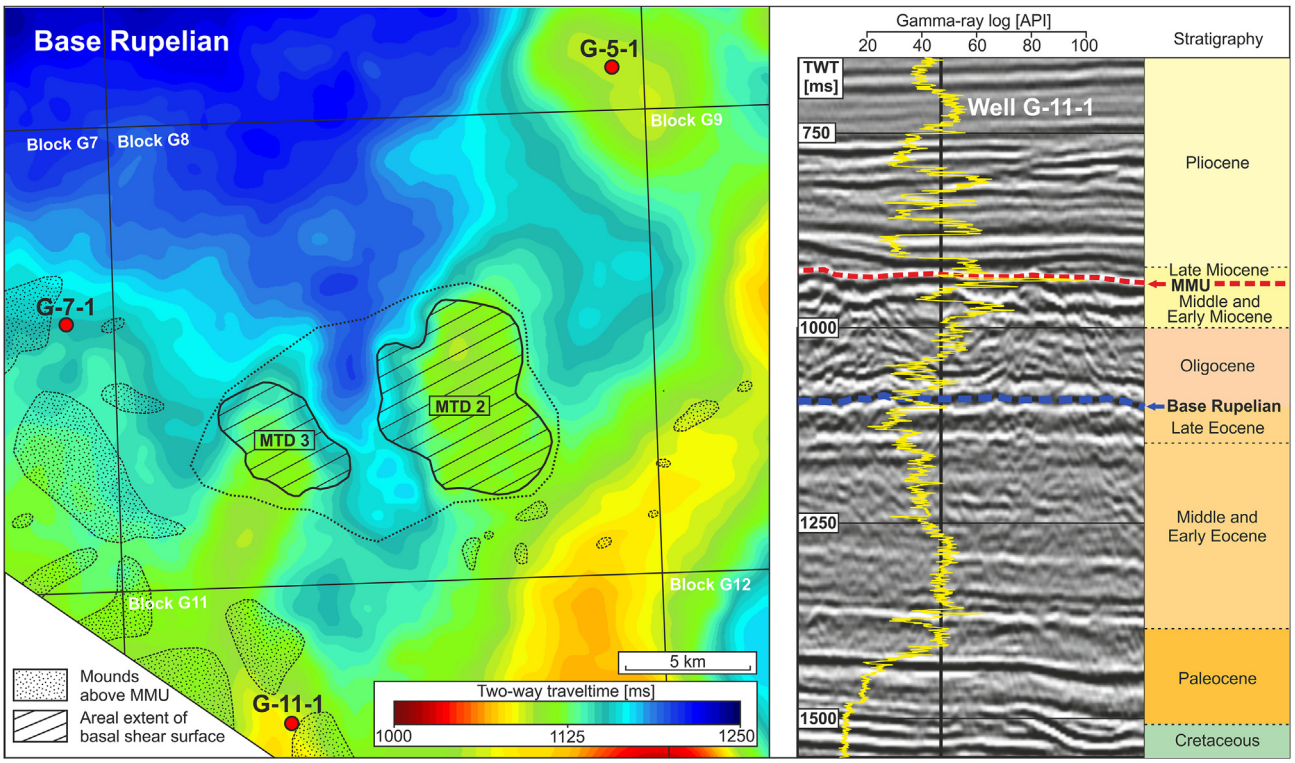

Fig. 8. Time-structure map of the base Rupelian within the vicinity of MTDs 2 and 3 (left panel). The base of the Rupelian acting as the main basal shear surface of MTDs 2 and 3 is locally uplifted by underlying salt structures, forming a positive structural relief associated with domal/anticlinal structures. Note that the detachment surface at the base of MTDs 2 and 3 is centered above the crests of topographic highs. Also marked are mounded structures found on top of the MMU as seen in Fig. 11. The mounds appear to be preferentially developed above underlying salt structures. The right panel shows a stratigraphic correlation between the gamma ray signature from well G-11-1 and seismic reflection data. Note that the base Rupelian separates intervals of varying polygonal-faulting and seismic amplitudes and that the intense faulted interval above the base Rupelian coincides with upward increasing gamma ray values.

we give priority to our newly determined age assessments and suggest that the MTDs of group 1 and 2 are Gelasian in age.

The MTDs in the German North Sea sector located East to the Dutch ones are found within seismic units SU3 (MTD 1) and SU6 (MTD 2 and 3) (Figs. 3 and 6). The stratigraphic position of the MTDs implies a Late Miocene (Late Tortonian) age for the oldest MTD 1 and a Piacenzian age for the younger MTDs 2 and 3 (Thöle et al., 2014, Table 1). The occurrence of older MTDs in the German North Sea sector compared to the Dutch ones is in accordance with the general direction of progradation (Fig. 12).

By examining the spatial and temporal distribution of the Dutch and German MTDs in a basin wide context a change in shelf margin stability can be observed. Progradation of the shelf margin started in the easternmost part of the German North Sea in the Late Tortonian (Thöle et al., 2014). The earliest slope failure (MTD1) occurred in the latest Tortonian. At this time, the shelf margin has already prograded more than 150 km to the west without any evidence for slope instabilities (Fig. 12), indicating a relatively stable slope during early margin growth. From the latest Tortonian until the end of the Pliocene, a period spanning more than 5 million years, the margin was only affected by two other slope failures (MTD 2 and 3). Whereas, in the Gelasian, which represents a time span of approximately 0.8 Ma, at least 30 slope failures occurred (Benvenuti et al., 2012). This shows that the return rate of slope failures increases significantly.

While the earliest slope failures of Late Miocene to Pliocene age in the German North Sea can be seen as more single events, the slope failures occurring later in the Pleistocene show higher frequencies and are more connected to each other. This suggests that the slope of the prograding system was apparently more stable during Late Miocene and Pliocene times, and that conditions changed in the basin after the Pliocene.

The increased occurrence of mass-transport processes in the area over time raises the questions: 1) what internal or external factors allowed the shelf margin to be susceptible to slope failure and 2) how do these factors have changed through time. Detailed analyses of the MTDs show that differences in the preconditions and triggers may have played an important role in the development of the MTD, which will be discussed in the following.

5.2. *Preconditions/possible trigger mechanisms for slope failure development*

The conditions leading to slope failures are difficult to elucidate and often form a complex pattern of interacting processes (Canals et al., 2004). Submarine slope failures generally initiate when the downslope-oriented shear stress exceeds the shear strength of the sediment. This can be the result of a downslope-oriented increase in shear stress, a reduction in sediment strength, or a combination of both (Hampton et al., 1996). Previous studies have identified numerous possible causes controlling the development of submarine slides along continental margins (e.g. Hampton et al., 1996; Hesthammer and Fossen, 1999; Hjelstuen et al., 2007; Leynaud et al., 2009; Frey-Martinez et al., 2011; Urlaub et al., 2013; Pattier et al., 2013). Some of these mechanisms may only prime the succession for failure (preconditions) with a separate mechanism acting as the trigger (Frey-Martinez et al., 2011). Potential preconditions to failure exist among others in the form of high sedimentation rates, unfavourable sediment layering, climate variability affecting sediment processes, oversteeping, and fluid

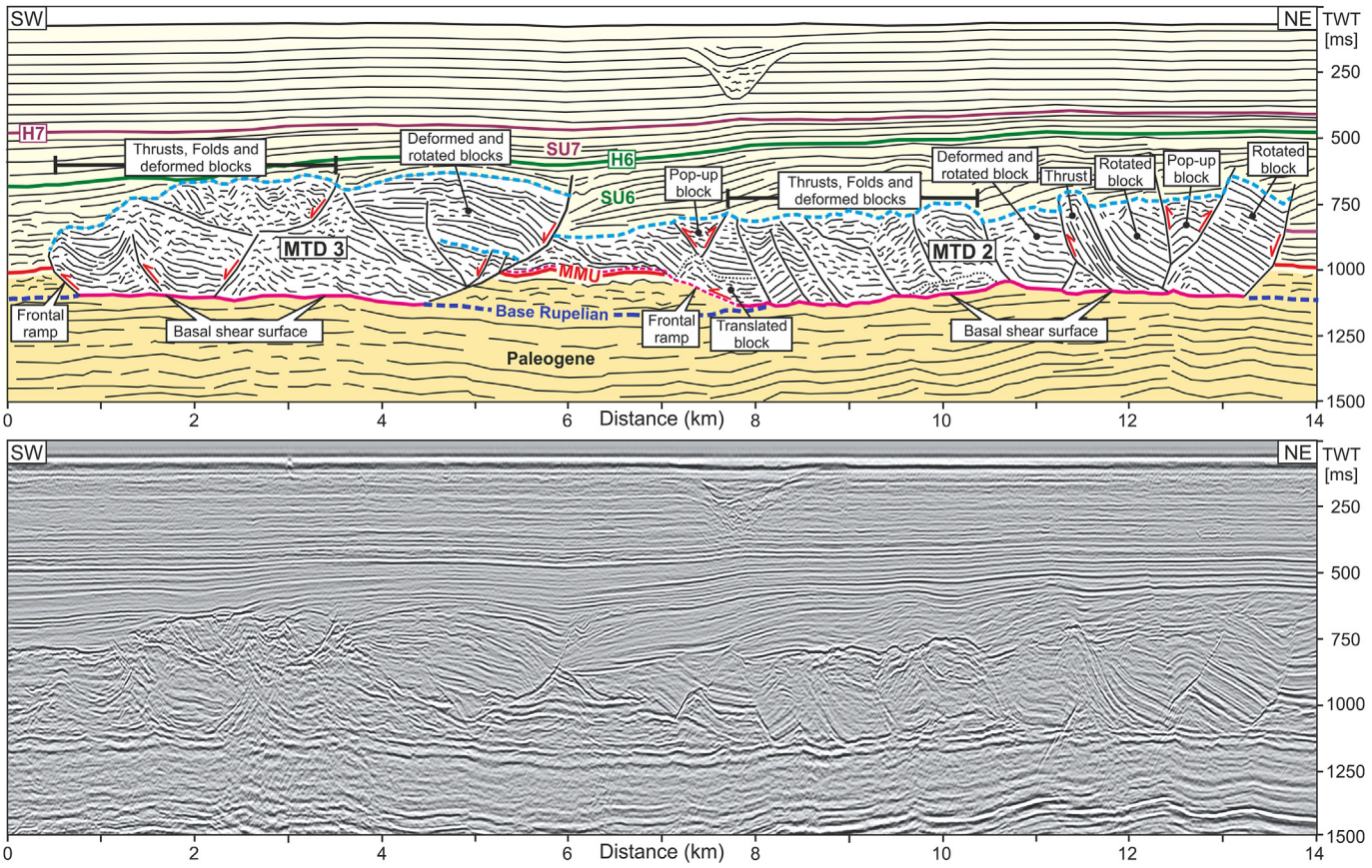

Fig. 9. Enlarged view of MTDs 2 and 3 shown in Fig. 6, illustrating the internal architecture of the MTDs. Note the difference in the toe regions of the MTDs. MTD 2 is characterized by a frontal ramp along which the displaced mass is translated above the paleo-seafloor, while MTD 3 has steep frontal ramp along which the displaced mass is buttressed against the undeformed stratigraphic section. Seismic data provided by TGS-NOPEC.

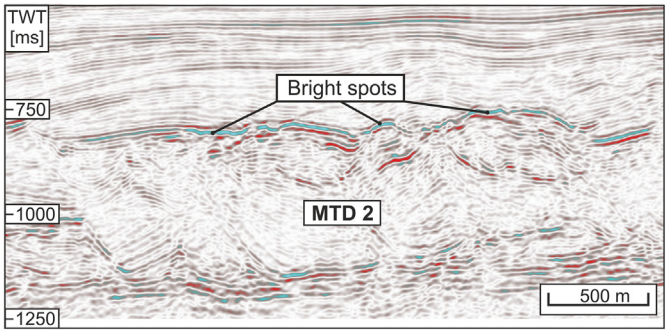

Fig. 10. Enlarged view of MTD 2 showing high-amplitude anomalies at the top of the MTD and also in part below its depositional area. These high amplitude anomalies characterized by distinct local brightening of the sedimentary reflections (bright spots) are probably caused by gas in the sediments. The location of the seismic profile is given in Fig. 6. Seismic data provided by TGS-NOPEC.

flow related factors (e.g. Vanneste et al., 2014). Seismicity is one of the most contemplated triggers for marine slope failures (e.g. Imbo et al., 2003; Gibert et al., 2005; Ingram et al., 2011).

Benvenuti et al. (2012) considered salt-induced seismicity, fluid migration as well as high-frequency sea level falls in combination with high sediment supply as possible factors that might have contributed to the release of slope failures in the Dutch North Sea sector. In the following we will place our findings from the German part of the North Sea in the context to the ones in the Dutch sector by considering the above mentioned mechanisms.

5.2.1. *Sediment supply and climate change*

Based on the strong prograding and down-stepping architecture of the clinoform system during slope failure formation Benvenuti et al. (2012) concluded that the main precondition for slope instability is high sediment supply in combination with a constant or even decreasing accommodation space (caused by constant or decreasing sea-level). This is in agreement with Overeem et al. (2001) who suggested that sea-level fall might have triggered slope failures along the shelf margin. The MTDs documented in this paper are also exclusively associated with units characterized by strongly prograding clinoforms with flat to low-angle ascending trajectories (i.e. SU3 and SU6), indicating limited or decreasing accommodation space on the shelf (Thöle et al., 2014). All analyses are based on mapping of seismic reflectors and horizons without considering the effects of compaction through back-stripping. The general lack of MTDs embedded in more aggradational units is in line with this. However, a direct link between strong progradational phases of the shelf margin and slope failure occurrences cannot solely be established.

Beside the markedly aggradational character of the shelf margin during early progradation (SU1 to SU2) and during Messinian (SU4) a strong progradational pattern characterized the clinoform system in the German North Sea during the remaining time, as shown by Thöle et al. (2014). Although the shelf margin predominantly exhibit a strong prograding character only three MTDs have been recognized within the German North Sea sector, whereas several slope failures have been identified within the Dutch part of the southern North Sea. Therefore, we assume that other factors than

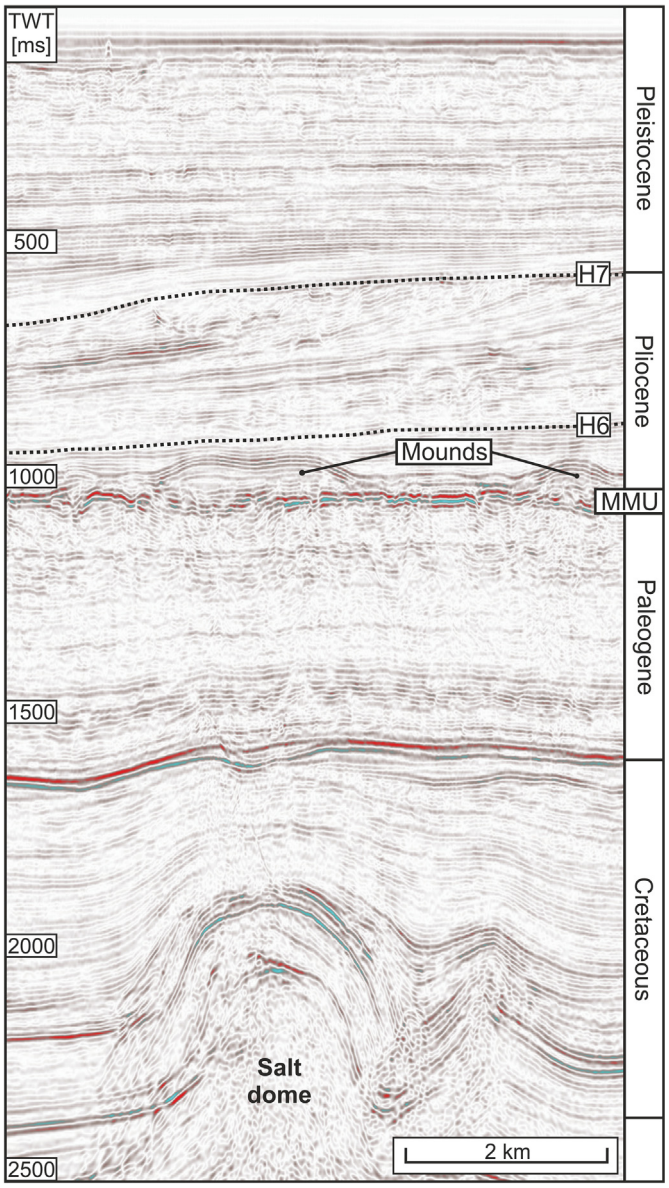

Fig. 11. Seismic section showing examples of mounded structures observed on top of the MMU and their clear spatial coincidence with underlying salt structures. In the vicinity of MTDs 2 and 3, numerous mounded structures have been identified lining up with underlying salt structures, as indicated in Fig. 8. Location of seismic profile is given in Fig. 2. Seismic data provided by TGS-NOPEC.

the combination of low accommodation and high sediment supply as proposed by Benvenuti et al. (2012) must have contributed to the release of slope failures in the southern North Sea.

In accordance to our chronostratigraphy, the change from a relatively stable shelf margin towards a margin affected by repeated slope failures coincides approximately with the onset of Northern Hemisphere Glaciations at ca. 2.75 Ma (Ravelo et al., 2004). From that time onward the frequency and intensity of climate variations increased significantly, as yielded by numerous deep-sea benthic foraminiferal $\delta^{18}O$ records (e.g. Ruddiman et al., 1989; Shackleton et al., 1990; Lisiecki and Raymo, 2005; Bell et al., 2014). Given the concurrent timing, glaciations and thus climate fluctuations may have played an important role for increased slope failure occurrences in the southern North Sea.

The effect of climate-driven environmental changes upon the occurrence and intensity of slope failure has been considered by several previous studies (e.g. Maslin et al., 2004; Bryn et al., 2005; Vanneste et al., 2006; Owen et al., 2007; Nelson et al., 2011). Climatically controlled alternations in sedimentation rate and type may affect the slope susceptibility to failure. Alternating sequences of glacial and interglacial deposits result in the formation of lithologically weak sediment layers which facilitate slope failure by serving as glide planes e.g., as reported offshore Norway (Laberg and Vorren, 2000) and in the Aegean Sea (Lykousis et al., 2002).

Kuhlmann and Wong (2008) demonstrate that from the Gelasian onward (~2.6 Ma ago) sedimentation in the southern North Sea was strongly influenced by glacier build-up and retreat, reflected in variations of sediment supply and type of sediments. One conspicuous feature of these alternations is, that during cold periods grain size was very fine (clayey) while during warm periods coarser-grained sediments were deposited (Kuhlmann and Wong, 2008). This has been explained by the interplay of glacial activity during cold periods and enhanced precipitation during warm periods (Kuhlmann, 2004). The resulting alternations of coarser grained (silty) sediments, having a higher porosity and finer grained (clayey) sediments, acting as seal apparently provides the potential for excess pore pressure build-up and thus reducing the sediment shear strength.

From the above mentioned it appears that the increased depositional variability associated with glacial-to-interglacial climatic cycles was an important precondition for the increased slope failure occurrences in the southern North Sea within the Pleistocene. Prior to the Pleistocene deposition took place under moderate to warm climatic conditions (Kuhlmann et al., 2006) and alternating sequences of glacial and interglacial deposits are not as abundant as in the Pleistocene succession (Fig. 13). This has profound consequences for the type of the basal shear surfaces. The basal shear surface of the Dutch MTDs is relatively shallow, commonly located at the base of a prograding clinoform or within a thin aggrading package at the basin floor (Benvenuti et al., 2012). The lithology around the level of detachment is usually associated with higher clay content (Benvenuti et al., 2012), probably related to the deposition during glacial periods in which sedimentation rate was relatively low (Kuhlmann and Wong, 2008). In the German North Sea failures occurred in contrast mainly along deeper stratigraphic level within the underlying Paleogene succession, as documented for MTDs 2 and 3 (Figs. 6 and 9). Therefore, other factors than alternations of glacial and interglacial deposits may have played a role in determining the position of the basal shear surface and thus the slope failure initiation in the German sector of the North Sea. These potential mechanisms will be discussed in more detail later.

Another climate-controlled factor that may have primed or triggered slope failure in the southern North Sea is glacio-eustatic sea-level fluctuation. Different effects of sea-level changes associated with glacial-and-interglacial phases have been addressed by several previous studies (e.g. Rothwell et al., 1998; Owen et al., 2007; Leynaud et al., 2009; Urlaub et al., 2013). According to Posamentier and Martinsen (2011) instability of slopes generally tends to preferentially favour relative low-stands of sea-level. They argued that during falling sea level the wave base is lowered, making the slopes more vulnerable to the effect of storm wave loading (Henkel, 1970; Suhayda et al., 1976). Benvenuti et al. (2012) considered this effect as a possible trigger for slope failure initiation.

Long-term sea level reconstructions, derived from marine oxygen isotope records (Fig. 13), indicate an overall fall in eustatic sea level from Mid-Miocene times onward caused by the onset of climatic cooling (e. g. Zachos et al., 2008; John et al., 2011; Miller et al., 2011). Through time the frequency and intensity of superimposed short-term sea level fluctuations increased significantly. In the Late

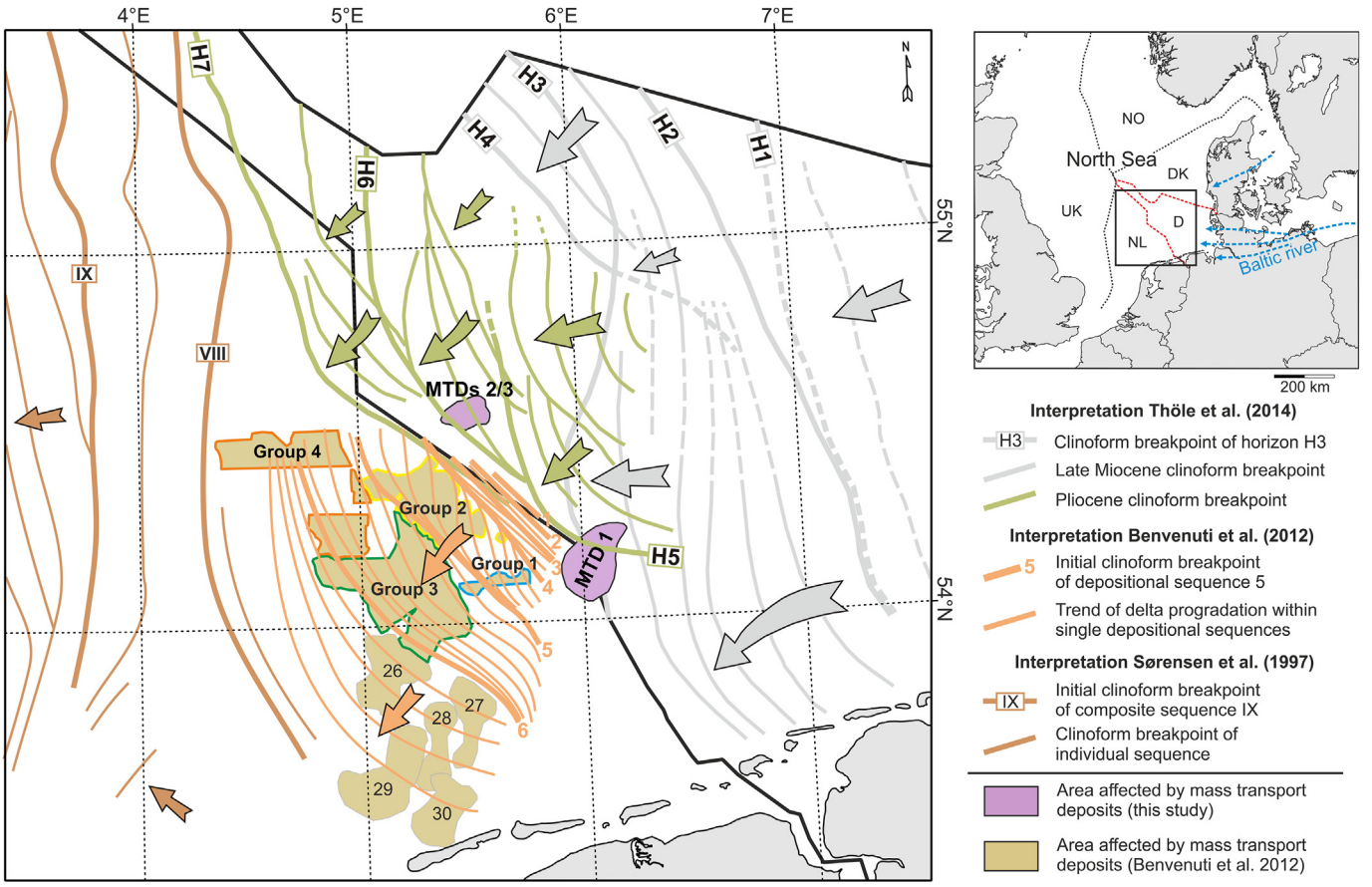

Fig. 12. Map showing the spatial distribution of Late Cenozoic MTDs in relation to shelf margin progradation as depicted from clinoform breakpoint lines (compiled from Sørensen et al., 1997; Benvenuti et al., 2012; Thöle et al., 2014).

Miocene to Late Pliocene, the amplitude of sea level changes were a few tens of meters at most, whereas during the Gelasian sea level changes showed higher frequencies with amplitudes up to 80 m (Miller et al., 2011, Fig. 13). The frequent sea level fluctuations with high amplitudes in the Pleistocene, reflecting episodes of global warming and cooling, and ice-sheet growth and decay, may have significantly increased the stress on the seafloor, making the slope susceptible for failure.

It seems that the development and deposition of the MTDs in the Dutch North Sea is clearly linked to climate-driven environmental changes. These are probably an increased stress on the seafloor due to high-frequency sea level fluctuations (trigger) as well as the depositional variability associated with glacial-to-interglacial climatic cycles (precondition). Prior to the Pleistocene potential failure mechanisms are preferably limited to those independent of glaciations and associated sea level changes and therefore less failures may have occurred. In the following we will discuss mechanisms that may have primed or triggered the older MTDs in the German North Sea, irrespective of climate-driven environmental changes.

5.2.2. *Salt structures and faults*

A large number of salt structures (pillows, walls and diapirs), belonging to the Rotliegend and Zechstein Group, are present in the southern North Sea Basin (e.g. Reinhold et al., 2008). These structures locally influenced the Cenozoic sedimentary succession (e.g. Korstgård et al., 1993; Remmelts, 1996: Brückner-Röhling et al., 2005), and are visible among others on the MMU (Fig. 1). Particular in the southern and southeastern part of the Dutch and German North Sea sectors, the MMU displays an irregular morphology with several circular to elongated highs, indicating post-Mid Miocene salt movements. Further to the north the MMU is less affected by underlying salt structures, as seen from their relatively smooth topography (Fig. 1).

The Late Miocene slope failure (MTD 1) described in this study as well as the younger MTDs 27 to 30 of Benvenuti et al. (2012) are located in the area severely affected by salt structures (Fig. 1). Due to the presence of headwall scars in proximity to salt-related faults, for instance for their MTD 27, Benvenuti et al. (2012) considered salt-induced seismicity as a possible trigger for slope failure. As evident from seismic section (Fig. 3), the oldest slope failure (MTD 1) was most likely also initiated by salt-related faulting. MTD 1 is located in relatively close proximity to salt diapirs, which influence the Late Cenozoic succession by synsedimentary faulting (Fig. 3). The normal faults offset sediment above the MTD, and offset decreases up section. This observation implies fault growth through various episodes of reactivation. Possibly, movement along these faults occurred in conjunction with the emplacement of the MTD, suggesting a direct connection between seismicity, faulting, and mass failure. Halokinetic movements are widely recognized as a common triggering mechanism for slope instabilities (e.g. Cashman and Popenoe, 1985; Popenoe et al., 1993; Tripsanas et al., 2003, 2004; Twichell et al., 2009).

In contrast, within the northern Dutch and German North sectors where the post-Mid Miocene succession is only gently affected by salt growth, halokinesis-induced seismicity is less likely. Since most MTDs are located in this area not affected by salt growth we suggest that salt-related seismicity may not be the primary driver

for slope failure development in the main part of the southern North Sea.

5.2.3. Excess pore pressure

Build-up of excess pore pressure (overpressured layers) and underconsolidation (weak layers) are often quoted as potential factors in causing instability (e.g. Imbo et al., 2003; Laberg et al., 2003; Canals et al., 2004; Flemings et al., 2008; Berndt et al., 2012). The generation of overpressure reduces the sediment strength, making it susceptible for failure (Stigall and Dugan, 2010). Overpressure can result from several mechanisms (Osborne and Swarbrick, 1997). For sedimentary basins in general, the most likely causes are compaction and hydrocarbon generation (Swarbrick et al., 2004). Regardless the process of overpressuring, it is proposed that physical properties of sediments are of primary importance in controlling pressure development in a basin (Frey-Martínez et al., 2006). As pointed out by Leynaud et al. (2007), permeability is a key factor in trapping excess pore pressure. An increase in pore pressure may result from the presence of relatively impermeable layers (seal), which prevent the expulsion of sufficient pore fluids of underlying sediments.

As discussed earlier, alternations of finer and coarser grained deposits accumulated during glacial and interglacial periods, respectively (Kuhlmann et al., 2006), could lead to build-up of excess pore pressure and may have played an important role in determining the position of the basal shear surface of the Pleistocene MTDs in the Dutch North Sea sector. The depth of a basal shear surface is mainly determined by the pressure gradient in the sediment and slippage along this surface occurs when pore pressure approaches or balances the normal stress of the overburden (Posamentier and Martinsen, 2011).

While the basal shear surface of MTD 1 and the MTDs in the Dutch North Sea sector is relatively shallow, commonly located at the base of a prograding clinoform or within a thin aggrading package at the basin floor (Benvenuti et al., 2012), the detachment surface at the base of MTDs 2 and 3 is located at a deeper stratigraphic level within the underlying Paleogene succession (Figs. 6 and 9). Therefore, other factors than alternations of glacial and interglacial deposits may have determined the position of the basal shear surface at the base of these MTDs. The mudstone-dominated Paleogene underlying the post-Mid Miocene sediments seem to be predestinated for overpressure generation and thus sliding along a weak layer.

Mudstones are one of the least permeable rocks; accordingly they can act as seals for fluid flow (Broichhausen et al., 2005). The permeability of mudstones, however, is strongly influenced by their mineralogical composition (Mondol et al., 2007), which may vary significantly within a succession. In our case, the exact lithology around the level of the detachment of MTD 2 and 3 is unknown, but it probably coincides with a change in lithology, most likely from a coarser grained into a muddier, lower permeable fine-grained lithology. The base Rupelian that acts as the basal shear surface separates intervals of varying polygonal-faulting and seismic amplitudes (Fig. 8). Dewhurst et al. (1999) pointed out that fault intensity correlates positively with both clay fraction and smectite content. The intense faulted interval above the base Rupelian may corresponds to a clay-rich interval with high smectite content. This interpretation is supported by observations from well logs from nearby wells (G-5-1, G-7-1 and G-11-1), which show upward increasing gamma values for this interval (Fig. 8).

Smectite-dominated clays have an extremely low permeability (Mondol et al., 2007). Therefore we assume that permeability barriers could have developed along this specific interval, which probably acts as a sealing succession in the study area. Fluid overpressure may build-up at the base of this regional seal, fostering subsequent slope failure.

The primary mechanism for overpressure generation in the Paleogene strata of the North Sea Basin is thought to be disequilibrium compaction, owing to the rapid rates of burial and sedimentation during Cenozoic times (Japsen, 1994). Vejbæk (2008) showed that the Upper Cretaceous – Paleogene succession of the Danish Central Graben becomes overpressured between the Late Miocene and the Holocene because of accelerated depositional rates. The position of MTDs commonly coincides with the main depocentre of the progradational units (Figs. 4 and 7). Rapid sediment accumulation in the German North Sea sector during Late Miocene to Late Pliocene (Thöle et al., 2014) might have also induced gradual but significant pore pressure generation below the prograding wedge in the Paleogene sediments. The increasing pore pressure lowers the strength of the sediments, leading to conditions that favour slope failure.

Another mechanism that may also contribute to overpressure generation at the location of MTDs 2 and 3 is the upward flow of water and hydrocarbons from deeper stratigraphic levels. MTDs 2 and 3 are located above two salt domes (Gracia in the west and Gloria in the east), which bent upwards the overlying sediments forming a positive structural relief associated with domal or anticlinal structures (Fig. 6). These structural highs combined with the presence of relatively impermeable layers covering this structure are favoured locations for fluid accumulations. Overpressure may have progressively increased within the sealed anticline due to upward migrating gas and fluids from deeper stratigraphic levels and thus decreasing the sediment strength, making the slope susceptible for failure.

Our suggestion of a deep fluid contribution to the overpressure development is mainly based on two observations (a) the widespread occurrence of fluid escape features represented by mounded structures on the MMU adjacent to the slope failures (Fig. 11), and the occurrence of probably gas-related seismic amplitude anomalies at the top and base of MTDs 2 and 3 (Fig. 10). The fact that the mounded structures as well as the seismic amplitude anomalies occur in close association with salt domes and/or faults suggests that fluids have migrated upward from deeper stratigraphic levels. Fluid migration was probably focused along the edge of salt diapirs, which are known to be locations of important fluid leakage in sedimentary basins (e.g. Cartwright et al., 2007). Accordingly to our observations Benvenuti et al. (2012) found similar mounded structures at their group 4 MTDs in the northern part of the slumping area implementing as well fluid involvement as possible trigger for these mass failures.

Upper Carboniferous coal measures and organic-rich shales, mainly of Namurian and Westphalian age, are believed to be the principal source rocks for hydrocarbons within the study area (Heim et al., 2013). Through petroleum system modeling, Heim et al. (2013) show that in the study area beneath our MTDs 2 and 3 Carboniferous source rocks were able to generate hydrocarbons from the Middle Permian onwards with a predominance of maturity increase during the Triassic until Late Jurassic.

For the present-day situation the model of Heim et al. (2013) shows no or only minor residual generation potential for the Carboniferous source rocks and no significant hydrocarbon accumulation within the study area. However, the upward migrated gas and fluid may have leaked from smaller reservoirs, which have been largely formed below the Rotliegend and Zechstein salt (Heim et al., 2013).

5.2.4. Conceptual model of the development of MTDs 2 and 3

Based on our interpretations presented above, a simple generic model for MTDs 2 and 3 is proposed that illustrate the process of slope failure and its controlling factors.

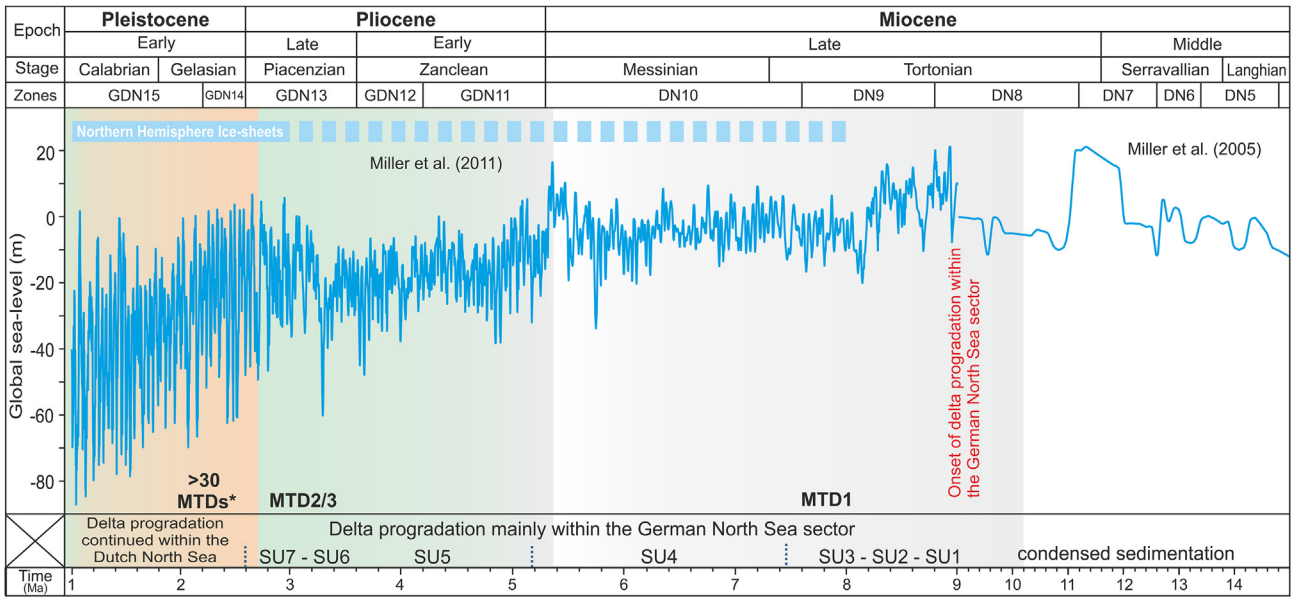

Fig. 13. Correlation of global sea level records for the past 9 Ma after Miller et al. (2011) and between 9 Ma and 15 Ma according to Miller et al. (2005) with the temporal occurrence of MTDs in the southern North Sea. Through time the frequency and intensity of superimposed short-term sea level fluctuations increased significantly. The frequent high-amplitudes sea level fluctuations within the Pleistocene, reflecting episodes of global warming and cooling, and ice-sheet growth and decay, coincide with increased frequency of slope failures. Dashed horizontal bars represent the development of northern hemisphere ice sheets, beginning in the late Miocene (~8 Ma) and reaching full glacial coverage (solid bar) during late Pliocene time (~3 Ma) after Zachos et al. (2001). The superimposed color shading is similar to the colors of the clinoform breakpoint lines shown in Fig. 12.

Fig. 14A depicts the initial situation before the onset of failure of MTD 2. Hydrocarbon leaking from deep reservoirs migrated vertically into the overlying Paleogene sediments. Fluid migration was focused along the edge of salt diapirs and upward migrating gas and fluid was trapped at the crest of salt-related anticlines. These structural highs combined with the presence of a relatively impermeable layer (interval between Base Rupelian and MMU) covering these structures were favoured locations for fluid accumulations. The low permeability interval prevents further upward migration and overpressure progressively increased at the top of the sealed anticlines. The increasing pore pressure lowers the strength of the sediments, leading to conditions that favour slope failure (Fig. 14A).

Instantaneous sediment loading during progradation rapidly increases the lithostatic stress of the overburden, which adds to already existing overpressures in the subsurface (Fig. 14A), and thus further reducing the sediment strength. If the reduction is large enough, most likely at the top of the sealed and overpressured anticline (location of highest expected overpressure), slope failure initiate (Fig. 14B). Away from the anticlinal trap, pore pressure gradients may remain normal and sediments are stable, and overlying strata may inherit their stability. The shelf margin remains stable until it reaches the next sealed and overpressured anticline in which pore pressure has been built up due to upward migrating fluid and finally in combination with loading imposed to the basin by the prograding wedge (Fig. 14C–D).

5.2.5. Comparison with global Cenozoic MTDs occurrences

One of the most striking observations from the present study is the change in shelf margin stability through time. The Late Cenozoic shelf margin in the southern North Sea developed from a relatively stable margin (Late Miocene to Pliocene) towards a margin affected by repeated slope failures (Pleistocene). Similar patterns are documented from various geographical locations worldwide, as for example along the western margin of the South Caspian Basin. Pliocene and older slopes were here apparently stable, with conditions changing in the basin after the Pliocene (Richardson et al., 2011). An enhanced slope failure activity in the Pleistocene is also observed along the continental margin of Israel (Eastern Mediterranean). Over 40 slump complexes have been identified within the post-Messinian succession of the southern Israeli continental margin by Frey-Martinez et al. (2005), whereby most of them were found above the Pliocene-Pleistocene boundary. Mass-wasting processes also become more common along the southwestern slope of Newfoundland during the Plio-Pleistocene. According to Giles et al. (2010), slope instability has been a recurrent process along the SW Newfoundland margin since at least the early Miocene. After the late Miocene, however, slope instabilities become more frequent, although the resulting products decreased in size (Giles et al., 2010). Numerous submarine slope failures of various sizes have been recognized within the Late Cenozoic succession along the NW European continental margin (Evans et al., 2005). Most of these mass-failure events took place during the mid-Pleistocene or later, during a period when a number of shelf-wide glaciations occurred. Nevertheless, a number of slope failures have already occurred intermittently since perhaps late Pliocene times, before significant glaciation (e.g. Evans et al., 2005; Hjelstuen and Andreassen, 2015; Safronova et al., 2015).

Several processes are assumed to affect the long-term stability of a margin (Vanneste et al., 2014). Our observations suggest that there is strong correlation between the Late Cenozoic climate deterioration, in particular the marked climate variability during the Pleistocene, and slope failure frequency. This finding is in general agreement with several other studies that have examined the impact of climate driven environmental changes on the occurrence and intensity of submarine slope failures during this time period (e.g. Owen et al., 2007). Likewise, the above-mentioned studies of Giles et al. (2010) and Richardson et al. (2011) considered climatic variations as a probable factor for the increased slope failure occurrences within the Pleistocene.

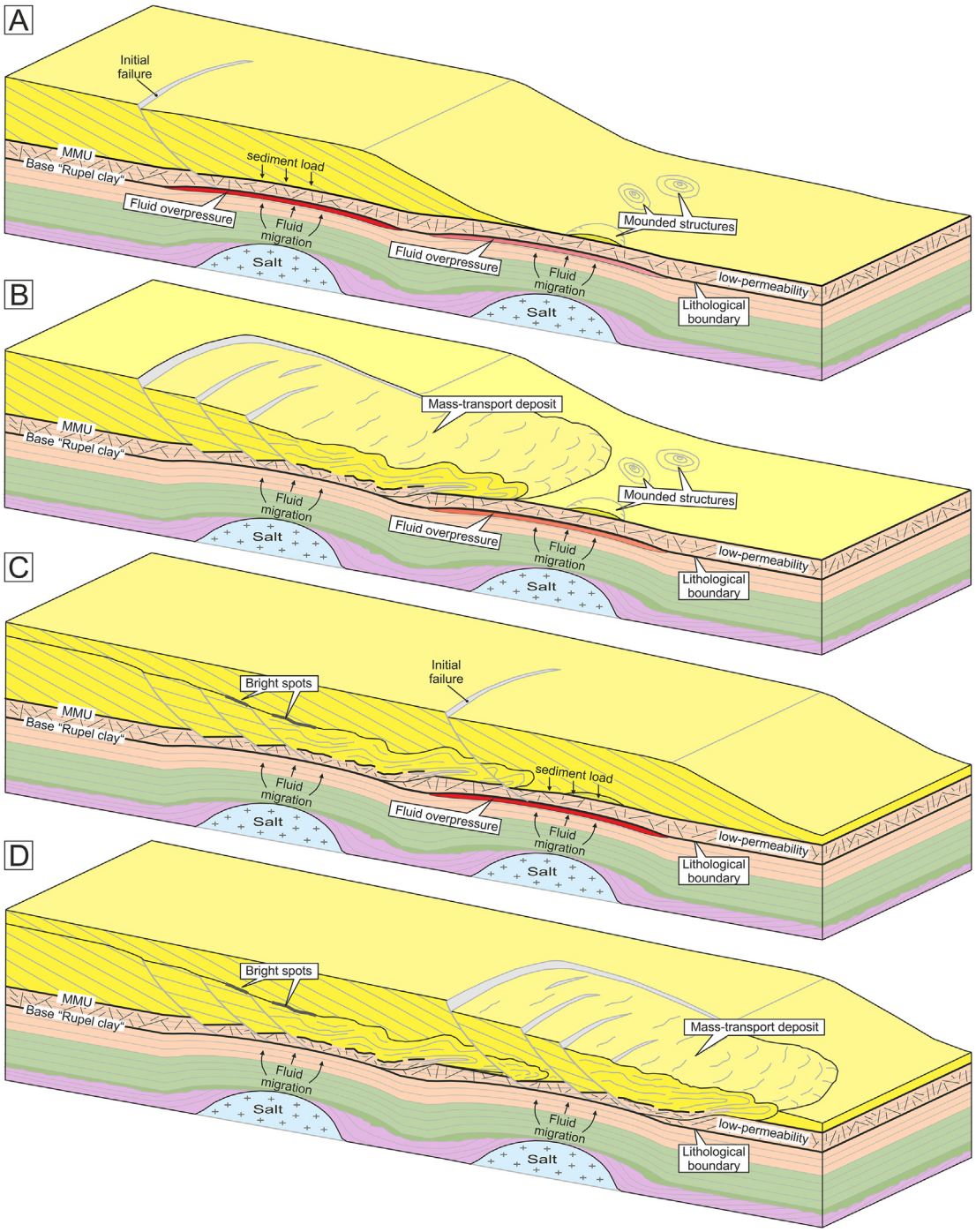

Fig. 14. Conceptual model of the development of MTDs 2 and 3 (not to scale). The different stages leading to slope failures on the shelf margin are described in the text.

6. Conclusions

The following conclusions can be drawn from this study:

- In the German part of the southern North Sea, three large mass transport deposits (MTDs) are observed within the Late Cenozoic sedimentary succession. They are the earliest in a series of slope failures that have affected the Late Cenozoic shelf margin in the southern North Sea during Late Miocene to Pleistocene times.
- The first slope failure (MTD 1) on the shelf margin occurred during Late Tortonian times, and is most likely triggered by salt-induced seismicity, as evident from salt-related faulting of the Late Cenozoic succession in its headwall domain.
- Two slope failures (MTDs 2 and 3) of apparently slightly differing age affected the westward prograding shelf margin during Piacenzian time. Excess pore pressure generation due to fluid migration from deeper stratigraphic levels in combination with loading imposed to the basin by the prograding wedge of the Late Cenozoic succession are interpreted as the main factors controlling these slope failures. Slippage occurred along the

crest of sealed and overpressured salt-related anticlines within the underlying Paleogene succession.

- Since early Pleistocene times there has been a distinct increase in shelf margin instabilities. The earliest slope failures that occurred during Late Miocene to Pliocene in the German part of the southern North Sea can be regarded as more individual events while the slope failures occurring later in the Pleistocene in the Dutch North Sea sector show much higher frequencies.
- The change from a relatively stable shelf margin towards a margin affected by repeated slope failures coincides approximately with the intensification of Northern Hemisphere Glaciations during Pleistocene times. The development and deposition of the MTDs in the Dutch North Sea is clearly linked to climate-driven environmental changes, whereas prior to the Pleistocene potential failure mechanisms are preferably limited to those independent of glaciations and associated sea level changes and therefore fewer failures have occurred.

Acknowledgements

We thank the companies organized in the industrial association WEG (Wirtschaftsverband Erdöl-und Erdgasgewinnung) and the companies BP and TGS-NOPEC for the permission to use their data sets for scientific research within this study. We also thank David Hodgson and an anonymous reviewer for their helpful and detailed comments, which helped to improve this article.

References

Andresen, K.J., Clausen, O.R., Huuse, M., 2009. A giant (5.3×10^7 m^3) middle Miocene (c. 15 Ma) sediment mound (M1) above the Siri Canyon, Norwegian–Danish Basin: origin and significance. Mar. Pet. Geol. 26, 1640–1655.
Bell, D.B., Jung, S.J.A., Kroon, D., Lourens, L.J., Hodell, D.A., 2014. Local and regional trends in Plio-Pleistocene δ18O records from benthic foraminifera. Geochem. Geophys. Geosystems 15, 3304–3321.
Benvenuti, A., Kombrink, H., ten Veen, J.H., Munsterman, D.K., Bardi, F., Benvenuti, M., 2012. Late Cenozoic shelf delta development and Mass Transport Deposits in the Dutch offshore area – results of 3D seismic interpretation. Neth. J. Geosci. 91, 591–608.
Berndt, C., Costa, S., Canals, M., Camerlenghi, A., de Mol, B., Saunders, M., 2012. Repeated slope failure linked to fluid migration: the Ana submarine landslide complex, Eivissa Channel, Western Mediterranean Sea. Earth Planet. Sci. Lett. 319–320, 65–74.
Bijlsma, S., 1981. Fluvial sedimentation from the Fennoscandian area into the Northwest European Basin during the Late Cenozoic. Geol. Mijnb. 8, 337–345.
Broichhausen, H., Littke, R., Hantschel, T., 2005. Mudstone compaction and its influence on overpressure generation, elucidated by a 3D case study in the North Sea. Int. J. Earth Sci. 94, 956–978.
Brückner-Röhling, S., Forsbach, H., Kockel, F., 2005. The structural development of the German North sea sector during the Tertiary and the Early Quaternary. Z. Dtsch. Ges. Geowiss. 156, 341–355.
Bryn, P., Berg, K., Forsberg, C.F., Solheim, A., Kvalstad, T.J., 2005. Explaining the Storegga Slide. Mar. Pet. Geol. 22, 11–19.
Bull, S., Cartwright, J., Huuse, M., 2009. A review of kinematic indicators from mass-transport complexes using 3D seismic data. Mar. Pet. Geol. 26, 1132–1151.
Bullimore, S.S., Henriksen, L.F.M., Helland-Hansen, W., 2005. Clinoform stacking patterns, shelf-edge trajectories and facies associations in Tertiary coastal deltas, offshore Norway. Implications for the prediction of lithology in prograding systems. Nor. J. Geol. 85, 169–187.
Callot, P., Odonne, F., Debroas, E.-J., Maillard, A., Dhont, D., Basile, C., Hoareau, G., 2009. Three-dimensional architecture of submarine slide surfaces and associated soft-sediment deformation in the Lutetian Sobrarbe deltaic complex (Ainsa, Spanish Pyrenees). Sedimentology 56, 1226–1249.
Cameron, T.D.J., Bulat, J., Mesdag, C.S., 1993. High resolution seismic profile through a Late Cenozoic delta complex in the southern North Sea. Mar. Pet. Geol. 10, 591–599.
Canals, M., Lastras, G., Urgeles, R., Casamor, J.L., Mienert, J., Cattaneo, A., De Batist, M., Haflidason, H., Imbo, Y., Laberg, J.S., Locat, J., Long, D., Longva, O., Masson, D.G., Sultan, N., Trincardi, F., Bryn, P., 2004. Slope failure dynamics and impacts from seafloor and shallow sub-seafloor geophysical data: case studies from the COSTA project. Mar. Geol. 213, 9–72.
Cartwright, J., Huuse, M., Aplin, A., 2007. Seal bypass systems. AAPG Bull. 91, 1141–1166.
Cartwright, J.A., 1994. Episodic basin-wide fluid expulsion from geopressured shale sequences in the North-Sea Basin. Geology 22, 447–450.
Cartwright, J.A., Lonergan, L., 1996. Volumetric contraction during the compaction of mudrocks: a mechanism for the development of regional-scale polygonal fault systems. Basin Res. 8, 183–193.
Cashman, K.V., Popenoe, P., 1985. Slumping and shallow faulting related to the presence of salt on the Continental Slope and Rise off North Carolina. Mar. Pet. Geol. 2, 260–271.
Dalla Valle, G., Gamberi, F., Rocchini, P., Minisini, D., Errera, A., Baglioni, L., Trincardi, F., 2013. 3D seismic geomorphology of mass transport complexes in a foredeep basin: examples from the Pleistocene of the Central Adriatic Basin (Mediterranean Sea). Sediment. Geol. 294, 127–141.
Deckers, J., 2015. Middle Miocene Mass Transport Deposits in the southern part of the Roer Valley Graben. Mar. Pet. Geol. 66 (Part 4), 653–659.
de Lugt, I.R., van Wees, J.D., Wong, T.E., 2003. The tectonic evolution of the southern Dutch North Sea during the Palaeogene: basin inversion in distinct pulses. Tectonophysics 373, 141–159.
Dewhurst, D.N., Cartwright, J.A., Lonergan, L., 1999. The development of polygonal fault systems by syneresis of colloidal sediments. Mar. Pet. Geol. 16, 793–810.
Domenico, S., 1976. Effect of brine-gas mixture on velocity in an unconsolidated sand reservoir. Geophysics 41, 882–894.
Dybkjær, K., Piasecki, S., 2010. Neogene dinocyst zonation for the eastern North Sea Basin, Denmark. Rev. Palaeobot. Palynol. 161, 1–29.
Eidvin, T., Riis, F., Rasmussen, E.S., 2014. Oligocene to Lower Pliocene deposits of the Norwegian continental shelf, Norwegian Sea, Svalbard, Denmark and their relation to the uplift of Fennoscandia: a synthesis. Mar. Pet. Geol. 56, 184–221.
Evans, D., Harrison, Z., Shannon, P.M., Laberg, J.S., Nielsen, T., Ayers, S., Holmes, R., Hoult, R.J., Lindberg, B., Haflidason, H., Long, D., Kuijpers, A., Andersen, E.S., Bryn, P., 2005. Palaeoslides and other mass failures of Pliocene to Pleistocene age along the Atlantic continental margin of NW Europe. Mar. Pet. Geol. 22, 1131–1148.
Flemings, P.B., Long, H., Dugan, B., Germaine, J., John, C.M., Behrmann, J.H., Sawyer, D., Scientists, I.E., 2008. Pore pressure penetrometers document high overpressure near the seafloor where multiple submarine landslides have occurred on the continental slope, offshore Louisiana, Gulf of Mexico. Earth Planet. Sci. Lett. 269, 309–325.
Fongngern, R., Olariu, C., Steel, R.J., Krézsek, C., 2015. Clinoform growth in a Miocene, Para-tethyan deep lake basin: thin topsets, irregular foresets and thick bottomsets. Basin Res. 1–26.
Frey-Martinez, J., Bertoni, C., Gérard, J., Matías, H., 2011. Processes of submarine slope failure and fluid migration on the Ebro Continental Margin: implications for offshore exploration and development. In: Shipp, R.C., Weimer, P., Posamentier, H.W. (Eds.), Mass-transport Deposits in Deepwater Settings. SEPM, pp. 181–198.
Frey-Martínez, J., 2010. 3D seismic interpretation of mass transport deposits: implications for basin analysis and geohazard evaluation. In: Submarine Mass Movements and Their Consequences – 4th International Symposium, pp. 553–568.
Frey-Martínez, J., Cartwright, J., James, D., 2006. Frontally confined versus frontally emergent submarine landslides: a 3D seismic characterisation. Mar. Pet. Geol. 23, 585–604.
Frey-Martinez, J., Cartwright, J., Hall, B., 2005. 3D seismic interpretation of slump complexes: examples from the continental margin of Israel. Basin Res. 17, 83–108.
Gibert, L., Sanz de Galdeano, C., Alfaro, P., Scott, G., López Garrido, A.C., 2005. Seismic-induced slump in Early Pleistocene deltaic deposits of the Baza Basin (SE Spain). Sediment. Geol. 179, 279–294.
Giles, M.K., Mosher, D.C., Piper, D.J.W., Wach, G.D., 2010. Mass Transport Deposits on the Southwestern Newfoundland Slope. In: Mosher, D., Shipp, R.C., Moscardelli, L., Chaytor, J., Baxter, C.P., Lee, H., Urgeles, R. (Eds.), Submarine Mass Movements and Their Consequences. Springer, Netherlands, pp. 657–665.
Glennie, K.W., Underhill, J.R., 2009. Origin, Development and Evolution of Structural Styles, Petroleum Geology of the North Sea. Blackwell Science Ltd., pp. 42–84
Glørstad-Clark, E., Birkeland, E.P., Nystuen, J.P., Faleide, J.I., Midtkandal, I., 2011. Triassic platform-margin deltas in the western Barents Sea. Mar. Pet. Geol. 28, 1294–1314.
Glørstad-Clark, E., Faleide, J.I., Lundschien, B.A., Nystuen, J.P., 2010. Triassic seismic sequence stratigraphy and paleogeography of the western Barents Sea area. Mar. Pet. Geol. 27, 1448–1475.
Gradstein, F.M., Ogg, J.G., Hilgen, F.J., 2012. On the geologic time scale. Newsl. Stratigr. 45, 171–188.
Hampton, M.A., Lee, H.J., Locat, J., 1996. Submarine landslides. Rev. Geophys. 34, 33–59.
Heim, S., Lutz, R., Nelskamp, S., Verweij, H., Kaufmann, D., Reinhardt, L., 2013. Geological evolution of the North Sea: cross-border Basin Modeling Study on the Schillground High. Energy Procedia 40, 222–231.
Helland-Hansen, W., Hampson, G.J., 2009. Trajectory analysis: concepts and applications. Basin Res. 21, 454–483.
Henkel, D.J., 1970. The role of waves in causing submarine landslides. Géotechnique 75–80.
Hesthammer, J., Fossen, H., 1999. Evolution and geometries of gravitational collapse structures with examples from the Statfjord Field, northern North Sea. Mar. Pet. Geol. 16, 259–281.
Hjelstuen, B.O., Eldholm, O., Faleide, J.I., 2007. Recurrent Pleistocene mega-failures on the SW Barents Sea margin. Earth Planet. Sci. Lett. 258, 605–618.
Hjelstuen, B.O., Andreassen, E.V., 2015. North Atlantic Ocean deep-water processes and depositional environments: a study of the Cenozoic Norway Basin. Mar. Pet. Geol. 59, 429–441.

Homza, T.X., 2004. A structural interpretation of the Fish Creek Slide (Lower Cretaceous), northern Alaska. AAPG Bull. 88, 265–278.
Imbo, Y., De Batist, M., Canals, M., Prieto, M.J., Baraza, J., 2003. The Gebra Slide: a submarine slide on the Trinity Peninsula Margin, Antarctica. Mar. Geol. 193, 235–252.
Ingram, W.C., Mosher, D.C., Sherwood, W.W., 2011. Biostratigraphy of an upper Miocene mass-transport deposit on Demerara Rise, northern South American margin. In: Shipp, R.C., Weimer, P., Posamentier, H.W. (Eds.), Mass-transport Deposits in Deepwater Settings. SEPM, pp. 475–497.
Japsen, P., 1994. Retarded compaction due to overpressure deduced from a seismic velocity/depth conversion study in the Danish Central Trough, North Sea. Mar. Pet. Geol. 11, 715–733.
Johannessen, E.P., Steel, R.J., 2005. Shelf-margin clinoforms and prediction of deepwater sands. Basin Res. 17, 521–550.
John, C.M., Karner, G.D., Browning, E., Leckie, R.M., Mateo, Z., Carson, B., Lowery, C., 2011. Timing and magnitude of Miocene eustasy derived from the mixed siliciclastic-carbonate stratigraphic record of the northeastern Australian margin. Earth Planet. Sci. Lett. 304, 455–467.
Kerr, R.S., 1985. Seismic expression of catastrophic slope failure: Lower Cretaceous Torok Formation, North Slope of Alaska. AAPG Bull. 69, 273.
Knox, R.W.O.B., Bosch, J.H.A., Rasmussen, E.S., Heilmann-Clausen, C., Hiss, M., De Lugt, I.R., Kasiński, J., King, C., Köthe, A., Słodkowska, B., Standke, G., Vandenberghe, N., 2010. Cenozoic. In: Doornenbal, J.C., Stevenson, A.G. (Eds.), Petroleum Geological Atlas of the Southern Permian Basin Area. EAGE Publications b.v., Houten, pp. 211–223.
Knutz, P.C., 2010. Channel structures formed by contour currents and fluid expulsion: significance for Late Neogene development of the central North Sea basin. In: Petroleum Geology Conference Series, vol. 7. Geological Society, London, pp. 77–94.
Korstgård, J.A., Lerche, I., Mogensen, T.E., Thomsen, R.O., 1993. Salt and fault interactions in the northeastern Danish Central Graben: observations and inferences. Bull. Geol. Soc. Den. 40, 197–255.
Köthe, A., 2007. Cenozoic biostratigraphy from the German North Sea sector (G-11-1 borehole, dinoflagellate cysts, calcareous nannoplankton). Z. Dtsch. Geol. Ges. 158 (2), 287–327.
Köthe, A., 2011. Biostratigraphie känozoischer Sedimente der Bohrungen B15-3, D1, G5–1, G11-1 und J5-1, Deutscher Nordsee Sektor. (Dinozysten und Kalknannoplankton) – Zusammenfassender Bericht, Hannover.
Kuhlmann, G., 2004. High Resolution Stratigraphy and Paleoenvironmental Changes in the Southern North Sea during the Neogene. An Integrated Study of Late Cenozoic Marine Deposits from the Northern Part of the Dutch Offshore Area. Faculty of Geosciences. Utrecht University, Utrecht, p. 209.
Kuhlmann, G., Langereis, C., Munsterman, D., Jan van Leeuwen, R., Verreussel, R., Meulenkamp, J., Wong, T.E., 2006. Chronostratigraphy of Late Neogene sediments in the southern North Sea Basin and paleoenvironmental interpretations. Palaeogeogr. Palaeoclimatol. Palaeoecol. 239, 426–455.
Kuhlmann, G., Wong, T.E., 2008. Pliocene paleoenvironment evolution as interpreted from 3D-seismic data in the southern North Sea, Dutch offshore sector. Mar. Pet. Geol. 25, 173–189.
Laberg, J.S., Vorren, T.O., 2000. The Trænadjupet Slide, offshore Norway — morphology, evacuation and triggering mechanisms. Mar. Geol. 171, 95–114.
Laberg, J.S., Vorren, T.O., Mienert, J., Haflidason, H., Bryn, P., Lien, R., 2003. Preconditions leading to the Holocene Trænadjupet Slide Offshore Norway. In: Locat, J., Mienert, J., Boisvert, L. (Eds.), Submarine Mass Movements and Their Consequences. Springer, Netherlands, pp. 247–254.
Leynaud, D., Mienert, J., Vanneste, M., 2009. Submarine mass movements on glaciated and non-glaciated European continental margins: a review of triggering mechanisms and preconditions to failure. Mar. Pet. Geol. 26, 618–632.
Leynaud, D., Sultan, N., Mienert, J., 2007. The role of sedimentation rate and permeability in the slope stability of the formerly glaciated Norwegian continental margin: the Storegga slide model. Landslides 4, 297–309.
L'Heureux, J.-S., Hansen, L., Longva, O., Emdal, A., Grande, L.O., 2009. A multidisciplinary study of submarine landslides at the Nidelva fjord delta, Central Norway – implications for geohazard assessment. Nor. J. Geol. 90, 1–20.
Lisiecki, L.E., Raymo, M.E., 2005. A Pliocene-Pleistocene stack of 57 globally distributed benthic δ18O records. Paleoceanography 20, PA1003.
Løseth, H., Rodrigues, N., Cobbold, P.R., 2012. World's largest extrusive body of sand? Geology 40, 467–470.
Lykousis, V., Roussakis, G., Alexandri, M., Pavlakis, P., Papoulia, I., 2002. Sliding and regional slope stability in active margins: North Aegean Trough (Mediterranean). Mar. Geol. 186, 281–298.
Maslin, M., Owen, M., Day, S., Long, D., 2004. Linking continental-slope failures and climate change: testing the clathrate gun hypothesis. Geology 32, 53–56.
McHugh, C.M.G., Damuth, J.E., Mountain, G.S., 2002. Cenozoic mass-transport facies and their correlation with relative sea-level change, New Jersey continental margin. Mar. Geol. 184, 295–334.
McHugh, C.M.G., Damuth, J.E., Gartner, S., Katz, M.E., Mountain, G.S., 1996. Oligocene to Holocene mass-transport deposits of the New Jersey continental margin and their correlation to sequence boundaries. In: Mountain, G.S., Miller, K.G., Blum, P.B., Poag, C.W., Twichell, D.C. (Eds.), Proc. ODP Sci. Results, vol. 150, pp. 189–228.
Michelsen, O., Thomsen, E., Danielsen, M., Heilmann-Clausen, C., Jordt, H., Laursen, G.V., 1998. Cenozoic Sequence Stratigraphy in the Eastern North Sea, Mesozoic and Cenozoic Sequence Stratigraphy of European Basins. SEPM (Society for Sedimentary Geology), pp. 91–118.
Miller, K.G., Kominz, M.A., Browning, J.V., Wright, J.D., Mountain, G.S., Katz, M.E., Sugarman, P.J., Cramer, B.S., Christie-Blick, N., Pekar, S.F., 2005. The Phanerozoic record of global sea-level change. Science 310, 1293–1298.
Miller, K.G., Mountain, G.S., Wright, J.D., Browning, J.V., 2011. A 180-million-year record of sea level and ice volume variations from continental margin and deep-sea isotopic records. Oceanography 24, 40–53.
Møller, L.K., Rasmussen, E.S., Clausen, O.R., 2009. Clinoform migration patterns of a Late Miocene delta complex in the Danish Central Graben; implications for relative sea-level changes. Basin Res. 21, 704–720.
Mondol, N.H., Bjørlykke, K., Jahren, J., Høeg, K., 2007. Experimental mechanical compaction of clay mineral aggregates—changes in physical properties of mudstones during burial. Mar. Pet. Geol. 24, 289–311.
Moscardelli, L., Wood, L., Mann, P., 2006. Mass-transport complexes and associated processes in the offshore area of Trinidad and Venezuela. AAPG Bull. 90, 1059–1088.
Nelson, C.H., Escutia, C., Damuth, J.E., Twichell, D.C., 2011. Interplay of mass-transport and turbidite-system deposits in different active tectonic and passive continental margin settings: external and local controlling factors. In: Shipp, R.C., Weimer, P., Posamentier, H.W. (Eds.), Mass-transport Deposits in Deepwater Settings. SEPM, pp. 39–66.
Osborne, M.J., Swarbrick, R.E., 1997. Mechanisms for generating overpressure in sedimentary basins; a reevaluation. AAPG Bull. 81, 1023–1041.
Overeem, I., Weltje, G.J., Bishop-Kay, C., Kroonenberg, S.B., 2001. The Late Cenozoic Eridanos delta system in the Southern North Sea Basin: a climate signal in sediment supply? Basin Res. 13, 293–312.
Owen, M., Day, S., Maslin, M., 2007. Late Pleistocene submarine mass movements: occurrence and causes. Quat. Sci. Rev. 26, 958–978.
Pattier, F., Loncke, L., Gaullier, V., Basile, C., Maillard, A., Imbert, P., Roest, W.R., Vendeville, B.C., Patriat, M., Loubrieu, B., 2013. Mass-transport deposits and fluid venting in a transform margin setting, the eastern Demerara Plateau (French Guiana). Mar. Pet. Geol. 46, 287–303.
Perov, G., Bhattacharya, J.P., 2011. Pleistocene shelf-margin delta: Intradeltaic deformation and sediment bypass, northern Gulf of Mexico. AAPG Bull. 95, 1617–1641.
Pinous, O.V., Levchuk, M.A., Sahagian, D.L., 2001. Regional synthesis of the productive Neocomian complex of West Siberia: sequence stratigraphic framework. AAPG Bull. 85 (10), 1713–1730.
Pletsch, T., Appel, J., Botor, D., Clayton, C.J., Duin, E.J.T., Faber, E., Górecki, W., Kombrink, H., Kosakowski, P., Kuper, G., Kus, J., Lutz, R., Mathiesen, A., Ostertag-Henning, C., Papiernek, B., Van Bergen, F., 2010. Cenozoic. In: Doornenbal, J.C., Stevenson, A.G. (Eds.), Petroleum Geological Atlas of the Southern Permian Basin Area. EAGE Publications b.v., Houten, pp. 225–253.
Popenoe, P., Schmuck, E.A., Dillon, W.P., 1993. The Cape Fear landslide: slope failure associated with salt diapirism and gas hydrate decomposition. In: Schwab, W.C., Lee, H.J., Twichell, D.C. (Eds.), Submarine Landslides: Selected Studies in the U.S. Exclusive Economic Zone. U. S. Geological Survey Bulletin 2002, Washington D.C., USA, pp. 40–53.
Posamentier, H.W., Martinsen, O.J., 2011. The character and genesis of submarine mass-transport deposits: insights from outcrop and 3D seismic data. In: Shipp, R.C., Weimer, P., Posamentier, H.W. (Eds.), Mass-transport Deposits in Deepwater Settings. SEPM, pp. 7–38.
Prior, D., Coleman, J., 1982. Active slides and flows in underconsolidated marine sediments on the slopes of the Mississippi Delta. In: Saxov, S., Nieuwenhuis, J.K. (Eds.), Marine Slides and Other Mass Movements. Springer, US, pp. 21–49.
Prior, D.B., Coleman, J.M., 1978. Disintegrating retrogressive landslides on very-low-angle subaqueous slopes, Mississippi delta. Mar. Geotechnol. 3, 37–60.
Rasmussen, E.S., 2009. Neogene inversion of the Central Graben and Ringkøbing-Fyn High, Denmark. Tectonophysics 465, 84–97.
Rasmussen, E.S., Vejbæk, O.V., Bidstrup, T., Piasecki, S., Dybkjær, K., 2005. Late Cenozoic depositional history of the Danish North Sea Basin: implications for the petroleum systems in the Kraka, Halfdan, Siri and Nini fields. In: Petroleum Geology Conference Series, vol. 6. Geological Society, London, pp. 1347–1358.
Ravelo, A.C., Andreasen, D.H., Lyle, M., Olivarez Lyle, A., Wara, M.W., 2004. Regional climate shifts caused by gradual global cooling in the Pliocene epoch. Nature 429, 263–267.
Reinhold, K., Krull, P., Kockel, F., 2008. Salzstrukturen Norddeutschlands. Bundesanstalt für Geowissenschaften und Rohstoffe. p. geologische Karte, Berlin/Hannover.
Remmelts, G., 1996. Salt tectonics in the southern North Sea, the Netherlands. In: Rondeel, H.E., Batjes, D.A.J., Nieuwenhuijs, W.H. (Eds.), Geology of Gas and Oil under the Netherlands. Springer, Netherlands, pp. 143–158.
Richardson, S.E.J., Davies, R.J., Allen, M.B., Grant, S.F., 2011. Structure and evolution of mass transport deposits in the South Caspian Basin, Azerbaijan. Basin Res. 23, 702–719.
Rothwell, R.G., Thomson, J., Kahler, G., 1998. Low-sea-level emplacement of a very large Late Pleistocene/'megaturbidite/' in the western Mediterranean Sea. Nature 392, 377–380.
Ruddiman, W.F., Raymo, M.E., Martinson, D.G., Clement, B.M., Backman, J., 1989. Pleistocene evolution: Northern hemisphere ice sheets and North Atlantic Ocean. Paleoceanography 4, 353–412.
Ryan, M.C., Helland-Hansen, W., Johannessen, E.P., Steel, R.J., 2009. Erosional vs. accretionary shelf margins: the influence of margin type on deepwater sedimentation: an example from the Porcupine Basin, offshore western Ireland. Basin Res. 21, 676–703.
Safronova, P.A., Laberg, J.S., Andreassen, K., Shlykova, V., Vorren, T.O., Chernikov, S.,

2015. Late Pliocene–early Pleistocene deep-sea basin sedimentation at high-latitudes: mega-scale submarine slides of the north-western Barents Sea margin prior to the shelf-edge glaciations. Basin Res. 1–19.
Shackleton, N.J., Berger, A., Peltier, W.R., 1990. An alternative astronomical calibration of the lower Pleistocene timescale based on ODP Site 677. Earth Environ. Sci. Trans. R. Soc. Edinb. 81, 251–261.
Sheriff, R.E., Geldart, L.P., 1995. Exploration Seismology, second ed. Cambridge University Press.
Sørensen, J.C., Gregersen, U., Breiner, M., Michelsen, O., 1997. High-frequency sequence stratigraphy of Upper Cenozoic deposits in the central and south-eastern North Sea areas. Mar. Pet. Geol. 14, 99–123.
Steel, R., Olsen, T., 2002. Clinoforms, clinoform trajectories and deepwater sands, sequence stratigraphic models for exploration and production. In: Evolving Methodology, Emerging Models, and Application Histories: 22nd Annual, v. 22. SEPM, pp. 367–380.
Stigall, J., Dugan, B., 2010. Overpressure and earthquake initiated slope failure in the Ursa region, northern Gulf of Mexico. J. Geophys. Res. Solid Earth 115, B04101.
Stuart, J.Y., Huuse, M., 2012. 3D seismic geomorphology of a large Plio-Pleistocene delta – 'Bright spots' and contourites in the Southern North Sea. Mar. Pet. Geol. 38, 143–157.
Suhayda, J.N., Whelan, T., Coleman, J.M., Booth, J.S., Garrison, L.E., 1976. Marine sediment instability: interaction of hydrodynamic forces and bottom sediments. In: Offshore Technology Conference Proceedings, pp. 129–140.
Swarbrick, R.E., Osborne, M.J., Yardley, G.S., 2004. Comparison of overpressure magnitude resulting from the main generating mechanisms. AAPG Mem. 1–12.
Thöle, H., Gaedicke, C., Kuhlmann, G., Reinhardt, L., 2014. Late Cenozoic sedimentary evolution of the German North Sea – a seismic stratigraphic approach. Newsl. Stratigr. 47, 299–329.
Tripsanas, E.K., Bryant, W.R., Phaneuf, B.A., 2004. Slope-instability processes caused by salt movements in a complex deep-water environment, Bryant Canyon area, northwest Gulf of Mexico. AAPG Bull. 88, 801–823.
Tripsanas, E.K., Bryant, W.R., Prior, D.B., Phaneuf, B.A., 2003. Interplay between salt activities and slope instabilities, Bryant Canyon Area, Northwest Gulf of Mexico. In: Locat, J., Mienert, J., Boisvert, L. (Eds.), Submarine Mass Movements and Their Consequences: 1st International Symposium. Springer Netherlands, Dordrecht, pp. 307–315.
Twichell, D.C., Chaytor, J.D., ten Brink, U.S., Buczkowski, B., 2009. Morphology of late Quaternary submarine landslides along the U.S. Atlantic continental margin. Mar. Geol. 264, 4–15.
Urlaub, M., Talling, P.J., Masson, D.G., 2013. Timing and frequency of large submarine landslides: implications for understanding triggers and future geohazard. Quat. Sci. Rev. 72, 63–82.
Vanneste, M., Mienert, J., Bünz, S., 2006. The Hinlopen Slide: a giant, submarine slope failure on the northern Svalbard margin, Arctic Ocean. Earth Planet. Sci. Lett. 245, 373–388.
Vanneste, M., Sultan, N., Garziglia, S., Forsberg, C.F., L'Heureux, J.-S., 2014. Seafloor instabilities and sediment deformation processes: the need for integrated, multi-disciplinary investigations. Mar. Geol. 352, 183–214.
Vejbæk, O.V., 2008. Disequilibrium compaction as the cause for Cretaceous–Paleogene overpressures in the Danish North Sea. AAPG Bull. 92, 165–180.
Vejbaek, O.V., Andersen, C., 1987. Cretaceous-Early Tertiary inversion tectonism in the Danish Central Trough. Tectonophysics 137, 221–238.
Westerhoff, W., 2009. Stratigraphy and Sedimentary Evolution. The Lower Rhine-meuse System during the Late Pliocene and Early Pleistocene (Southern North Sea Basin). Vrije Universiteit Amsterdam, p. 168.
Zachos, J.C., Dickens, G.R., Zeebe, R.E., 2008. An early Cenozoic perspective on greenhouse warming and carbon-cycle dynamics. Nature 451, 279–283.
Zachos, J., Pagani, M., Sloan, L., Thomas, E., Billups, K., 2001. Trends, rhythms, and aberrations in global climate 65 Ma to present. Science 292, 686–693.
Ziegler, P.A., 1990. Tectonic and palaeogeographic development of the North Sea rift system. In: Blundell, D.J., Gibbs, A.D. (Eds.), Tectonic Evolution of the North Sea Rifts. Oxford Science Publications, Oxford, pp. 1–36.
Ziegler, P.A., 1992. North Sea rift system. Tectonophysics 208, 55–75.